Biochimica et Biophysica Acta 1843 (2014) 985–1001

Contents lists available at ScienceDirect

Biochimica et Biophysica Acta

journal homepage: www.elsevier.com/locate/bbamcr

Nucleocytoplasmic shuttling of the Duchenne muscular dystrophy gene product dystrophin Dp71d is dependent on the importin α/β and CRM1 nuclear transporters and microtubule motor dynein ☆

R. Suárez-Sánchez [a,b], A. Aguilar [a], K.M. Wagstaff [c], G. Velez [a], P.M. Azuara-Medina [a], P. Gomez [a], A. Vásquez-Limeta [a], O. Hernández-Hernández [b], K.G. Lieu [c], D.A. Jans [c,**,1], B. Cisneros [a,*,1]

[a] Departamento de Genética y Biología Molecular, Centro de Investigación y Estudios Avanzados del Instituto Politécnico Nacional (CINVESTAV-IPN), México D.F, Mexico
[b] Laboratorio de Medicina Genómica, Departamento de Genética, Instituto Nacional de Rehabilitación, México D.F, Mexico
[c] Nuclear Signalling Laboratory, Department of Biochemistry and Molecular Biology, Monash University, Clayton, VIC, Australia

ARTICLE INFO

Article history:
Received 4 May 2013
Received in revised form 17 December 2013
Accepted 24 January 2014
Available online 30 January 2014

Keywords:
Dystrophin Dp71
Importins
Exportin Crm1
ZZ domain
Dynein
Emerin

ABSTRACT

Even though the Duchenne muscular dystrophy (DMD) gene product Dystrophin Dp71d is involved in various key cellular processes through its role as a scaffold for structural and signalling proteins at the plasma membrane as well as the nuclear envelope, its subcellular trafficking is poorly understood. Here we map the nuclear import and export signals of Dp71d by truncation and point mutant analysis, showing for the first time that Dp71d shuttles between the nucleus and cytoplasm mediated by the conventional nuclear transporters, importin (IMP) α/β and the exportin CRM1. Binding was confirmed in cells using pull-downs, while *in vitro* binding assays showed direct, high affinity (apparent dissociation coefficient of c. 0.25 nM) binding of Dp71d to IMPα/β. Interestingly, treatment of cells with the microtubule depolymerizing reagent nocodazole or the dynein inhibitor EHNA both decreased Dp71d nuclear localization, implying that Dp71d nuclear import may be facilitated by microtubules and the motor protein dynein. The role of Dp71d in the nucleus appears to relate in part to interaction with the nuclear envelope protein emerin, and maintenance of the integrity of the nuclear architecture. The clear implication is that Dp71d's previously unrecognised nuclear transport properties likely contribute to various, important physiological roles.

1. Introduction

Duchenne muscular dystrophy (DMD) is a progressive and lethal X-linked inherited neuromuscular disorder that results, in the majority of cases, from large out-of-frame deletions or duplication in the *DMD* gene leading to absence or dysfunction of the dystrophin protein [1,2]. The *DMD* gene exhibits complex transcriptional regulation; it drives the synthesis of a variety of dystrophin isoforms through alternative internal promoters. Full-length dystrophin (427 kDa) is derived from three independent promoters at the 5′-end of the *DMD* gene [3,5], while the N-terminally truncated dystrophin variants Dp260, Dp140, Dp116, and Dp71 are produced from alternative internal promoters [6,9].

The shortest *DMD* gene product, Dp71, is also expressed in a wide variety of non-muscle tissues [7,10,11]; however, its levels vary greatly between different tissue and cell types, as well as during differentiation, *via* tight regulation of Dp71 promoter activity [12,13]. In similar fashion to full-length dystrophin in skeletal muscle, Dp71 associates with dystrophin associated proteins (DAPs) such as dystroglycans, sarcoglycans, dystrobrevins, syntrophins, and accessory proteins to form the Dystrophin-associated protein complex (DAPC) in non-muscle tissues. DAPC serves as a bridge to connect the extracellular matrix to the cytoskeleton, providing structural stability to the plasma membrane, and modulating cell signalling events across it [1]. Since Dp71 is the most abundant *DMD* gene product in adult brain [1,7,14] and because DMD patients with mutations located in the Dp71 genomic region display severe mental retardation ([15,16], reviewed in [17]), loss-of-function of Dp71 has emerged as a major contributing factor to cognitive impairment in DMD patients. Furthermore, the involvement of Dp71 in various different cellular processes, including ion and water homeostasis [18,19], cell adhesion [20,22], cell cycle division [23] and maintenance

☆ Contract grant sponsors: CONACyT (Mexico); Contract grant number: 128418 to BC. The National Health and Medical Research Council (Australia); Contract grant number: APP1002486 to DAJ.

* Correspondence to: B. Cisneros, Av. IPN 2508, Col. San Pedro Zacatenco, Deleg. Gustavo A. Madero, 07360 Mexico City, Mexico. Tel.: +52 55 5061 3339; fax: +52 55 5061 3931.
** Correspondence to: D.A. Jans, Department of Biochemistry and Molecular Biology, Building 77, Monash University, Monash, VIC 3800, Australia. Tel.: +61 3 9902 9341; fax: +61 3 9905 9500.
E-mail addresses: david.jans@monash.edu (D.A. Jans), bcisnero@cinvestav.mx (B. Cisneros).
[1] These authors contributed equally to this study.

0167-4889/$ – see front matter © 2014 Elsevier B.V. All rights reserved.
http://dx.doi.org/10.1016/j.bbamcr.2014.01.027

of nuclear architecture [24,25] has been reported in cultured cells as well as murine models.

In spite of being initially described as a cytoplasmic/plasma membrane-associated protein, Dp71 has been found in the nucleus of a number of different cell types, including hippocampal neurons, forebrain astrocytes, as well as in cell lines such as PC12, HeLa, and C2C12 [24,27]. Interestingly, alternative splicing of exon 78 of Dp71 results in several different isoforms of the protein that show differential subcellular localisation. Dp71d, for example, includes the domains encoded by exons 78 and 79 and exhibits a predominant nuclear localisation, while Dp71f, a variant harboring an alternative 31 amino acid C-terminal domain, through removal of exon 78, is exclusively cytoplasmic [28,30]. The molecular mechanisms modulating the nuclear translocation of Dp71d, however, remain to be defined.

Nuclear import and export of proteins >~40 kDa is highly regulated in eukaryotic cells. Nuclear import is conventionally dependent on the recognition of nuclear localisation signals (NLSs) by members of the importin (IMP) superfamily of proteins, of which there are multiple α and β forms. Nuclear export is an analagous process that requires nuclear export signals (NESs), which are recognised by exportins, a subset of IMPβ homologues [31,32]. In the present study, we characterize the nuclear transport pathway of Dp71d for the first time. We identify functional NLS and NES motifs that are responsible for nucleocytoplasmic shuttling of Dp71d and demonstrate that Dp71d's nuclear import is mediated by IMPα/β1, while its nuclear export is dependent on exportin-1/CRM1. Intriguingly, Dp71d nuclear import also appears to be facilitated by microtubules and the motor protein dynein. We also show for the first time that the role of Dp71d in the nucleus appears to relate to interaction with the nuclear envelope protein emerin, and maintenance of the integrity of the nuclear architecture. The results shed important light on how Dp71d can enter/exit the nucleus, to fulfil its various diverse roles in the cell.

2. Materials and methods

2.1. Plasmid constructs

Encoding sequence of mouse Dp71d was amplified by PCR using pRcCMV2-Dp71d [33] as the template, and the oligonucleotides described in Table 1. The PCR fragment was then inserted in frame into *Eco*RI-digested plasmids pGEX-4 T1 (Amersham Bioscience, GE Healthcare, Buckinghamshire, UK) for expression of GST-Dp71d fusion protein in bacteria, or pEGFP–N1 vector (Clontech Laboratories, Inc.) for expression of GFP-Dp71d protein fusion in eukaryotic cells. For analysis in transfected mammalian cells of full-length Dp71d and its truncation derivatives fused to TetraGFP, the respective cDNA fragments (full-length, Amino, Carboxyl, AminoΔZZ and ZZ) were amplified by PCR from the pRcCMV-Dp71d vector using the appropriate oligonucleotides (see Table 1). PCR fragments flanked by *Eco*RI sites were digested and cloned in frame into plasmid pTetraGFP [34], which encodes for four GFP in tandem, and has a multiple cloning site between the third and the fourth GFP. pSG5-Emerin vector was generated for *in vitro* binding assays of Dp71d with emerin. The coding sequence of human emerin was amplified by PCR from HeLa cell cDNA using the oligonucleotide primers described in Table 1, and the PCR fragment then digested and inserted in frame into *BamH1*-digested plasmid pSG5 vector.

Mutant variants of the ZZ domain of Dp71d, containing single [ZZ-1 (H241A), ZZ-2 (C251A), ZZ-3 (H263A), ZZ-4 (C272A)] or combined [ZZ-5 (C251A and H263A)] mutations in the zinc-chelating amino acid residues, and the Dp71d NES derivative mutant (NES mut) were generated by site-directed mutagenesis using the pTetraGFP-ZZ and pGFP-Dp71d vectors as templates respectively, and the oligonucleotides listed in Table 1. Briefly, 50 ng of the plasmid (pTetraGFP-ZZ or pGFP-Dp71d) were used in a PCR reaction containing 0.5 μl of Herculase II Fusion

Table 1
Oligonucleotides used in this study. Mutant codons are denoted by bold letters.

Assay	Vector/mutant	Oligonucleotide sequence
Cloning	pGEX4T1-Dp71	Forward 5′-A GTC GAA TTC ATG AGG GAA CAG CTC AAA GG-3′ Reverse 5′-A GTC GAA TTC CTA CAT TGT GTC CTC TCT CAT-3′
	pEGFPN1-Dp71	Forward 5′-A GTC GAA TTC ATG AGG GAA CAG CTC AAA GG-3′ Reverse 5′-A GTC GAA TTC TCA TTG TGT CCT CTC TCA T-3′
	pTetraGFP-Dp71	Forward 5′-AG TCG AAT TCT ATG AGG GAA CAG CTC AAA GG-3′ Reverse 5′-AGT CGA ATT CTT CAT TGT GTC CTC TCT CAT-3′
	pTetraGFP-Amino	Forward 5′-AG TCG AAT TCT ATG AGG GAA CAG CTC AAA GG-3′ Reverse 5′-AGT CGA ATT CCC CGT TTC CAT GTT GTC CCC CTC-3′
	pTetraGFP-Carboxyl	Forward 5′-AG TCG AAT TCT TGT GGA ATA TTG CAC TCC GA-3′ Reverse 5′-AGT CGA ATT CTT CAT TGT GTC CTC TCT CAT-3′
	pTetraGFP-ZZCarboxyl	Forward 5′-AG TCG AAT TCA GAG TGG CTG CTG CAG AAA CT-3′ Reverse 5′-AGT CGA ATT CTT CAT TGT GTC CTC TCT CAT-3′
	pTetraGFP-AminoΔZZ	Forward 5′-AG TCG AAT TCT ATG AGG GAA CAG CTC AAA GG-3′ Reverse 5′-AGT CGA ATT CCT TCT GTG CAG GAC GGG CAG CCA-3′
	pTetraGFP-ZZ	Forward 5′-AG TCG AAT TCT AGA GTG GCT GCT GCA GAA ACT-3′ Reverse 5′-AGT CGA ATT CCC CGT TTC CAT GTT GTC CCC CTC-3′
	pGEX4T1-ZZ	Forward 5′-AG TCG AAT TCA GAG TGG CTG CTG CAG AAA CT-3′ Reverse 5′-AGT CGA ATT CCC CGT TTC CAT GTT GTC CCC CTC-3′
	pSG5-Emerin	Forward 5′-ACTGGATCCATGGACAACTACGCAGATCT-3′ Reverse 5′-ACTGGATCCCTAGAAGGGGTTGCCTTCT-3′
Cloning by BP recombination	pDEST17-ZZ	Forward 5′-GGGGACAAGTTTGTACAAAAAAGCAGGCGTGGCTGCTGCAGAAACTGC-3′ Reverse 5′-GGGGACCACTTTGTACAAGAAAGCTGGGTTCACGTTTCCATGTTGTCCCCCTC-3′
Mutagenesis	ZZ-1	Forward 5′-GAA ACT GCC AAG **GC**T CAG GCC AAA TG-3′ Reverse 5′-CA TTT GGC CTG A**GC** CTT GGC AGT TTC-3′
	ZZ-2	Forward 5′-C ATC TGC AAA GAG **GC**T CCA ATC ATT G-3′ Reverse 5′-C AAT GAT TGG A**GC** CTC TTT GCA GAT G-3′
	ZZ-3	Forward 5′-C AGG AGT CTA AAG **GC**C TTT AAT TAT G-3′ Reverse 5′-C ATA ATT AAA G**GC** CTT TAG ACT CCT G-3′
	ZZ-4	Forward 5′-AC ATC TGC CAA AGC **GC**C TTT TTT TCT G-3′ Reverse 5′-C AGA AAA AAA G**GC** GCT TTG GCA GAT GT-3′
	ZZ-5	ZZ-2 and ZZ-3 combined
	NES mut	Forward 5′-G GAG TCA CAG **GCA** CAC AGG **GCA** AGG CAG **GCG** CTG GAG CAA CC-3′ Reverse 5′-GG TTG CTC CAG **CGC** CTG CCT **TGC** CCT GTG **TGC** CTG TGA CTC C-3′

DNA polymerase (Agilent Technologies, Santa Clara, CA, USA), 1× Herculase II reaction buffer, 0.2 mM dNTPs, 10 pmol of each oligonucleotide and water to 50 μl. Following temperature cycling, DpnI treatment was performed to cleave parental DNA and to improve the efficiency of the mutant plasmid screening. The reaction was transferred into Top10 competent cells, and the transformation mixture was plated on LB kanamycin plates. Plasmid integrity was confirmed in all cases by DNA sequencing.

The plasmid construct for bacterial expression of the ZZ domain of Dp71d fused to His6-tag was generated using the Gateway™ system (Invitrogen, Carlsbab, CA, USA). The DNA fragment encoding the ZZ domain was amplified by PCR using primers containing attB1 and attB2 recombination sites (Table 1). The PCR fragment was recombined into the pDONOR207 vector *via* the BP recombination reaction and the resulting plasmid, pDONOR207-ZZ, was then used to perform an LR recombination reaction with the prokaryotic expression vector pDEST17 to generate pDEST17-ZZ plasmid. The integrity of the construct was verified by DNA sequencing. Expression vectors encoding His6-tagged GFP alone as well as GST (glutathione S-transferase) alone or fused to mouse IMPα2 and β1 have been previously described [35,36]. The plasmid encoding DsRed-RanQ69L (DsRed-dominant negative mutant of Ran) was provided by Michael Green [37].

2.2. Antibodies

The following primary antibodies were used: +78Dp71 (Genemed Synthesis Inc. San Francisco, CA, USA) [25] and WB78 (Washington Biotechnology, Inc., Baltimore, USA), rabbit polyclonal antibodies directed against the C-terminal 13 amino acids of dystrophin. Rabbit polyclonal antibodies directed against IMPα2 (B-9), IMPβ2 (A-11), α-tubulin (B-7), emerin (FL-254) (Santa Cruz Biotechnology, Santa Cruz, CA., USA); IMPβ1 (3E9) (Abcam, Cambridge, UK); and a mouse monoclonal antibody that recognizes the central domain of actin [38], kindly provided by Dr. Manuel Hernández from CINVESTAV-IPN.

2.3. Tissue culture and transfection

Cells from the C2C12, HTC and PC12 cell lines, as well as the PC12 derivative clone AS1-Dp71, were grown as previously [25,27,39]. Where indicated, cells were subjected to various treatments. These included incubation for 24 h with the zinc chelator agent N,N,N′,N′-Tetrakis-(2-pyridylmethyl)-ethylenediamine (TPEN; Sigma-Aldrich, St Louis, Missouri, USA) at 1.1 μM, or for 4 h with 20 μg/ml cytochalasin B (Sigma-Aldrich, St Louis, Missouri, USA) or for 5 h with 5 μg/ml nocodazole (Sigma-Aldrich, St Louis, Missouri, USA) to disrupt the cytoskeleton. For inhibition of nuclear protein import or export, cells were treated with 20 μg/ml *Agaricus Bisporus* lectin (ABL, from edible mushroom; Sigma-Aldrich, St Louis, Missouri, USA) for 24 h or 100 ng/ml Leptomycin B (LMB; Sigma-Aldrich, St Louis, Missouri, USA) for 24 or 12 h. Kinesin and dynein were inhibited by incubation for 12 h with 10 μM aurintricarboxylic acid (AA; Sigma-Aldrich, St Louis, Missouri, USA) or with 1 mM erythro-9-(2-hydroxy-3-nonyl) adenine (EHNA; Sigma-Aldrich, St Louis, Missouri, USA), respectively. Cells were transfected using lipofectamine 2000 (Invitrogen, Carlsbad, California, USA), following the provider's protocol, and analysed 24 h post-transfection. Where the role of Ran was tested, cells were transfected to express dsRed-RanQ69L, a dominant-negative Ran mutant that is locked in the GTP-bound conformation and thus inhibits IMP-dependent nuclear protein import [37].

2.4. Immunofluorescence and confocal laser scanning microscopy

Cells plated on coverslips were fixed and permeabilized following standard procedures, and incubated overnight at 4 °C with the anti-Dp71 antibody WB78 (Washington Biotechnology, Inc., Baltimore, USA). Cells were then washed with PBS and incubated for 1 h at room temperature with a fluorescein-conjugated goat anti-rabbit IgG (Zymed Laboratories, Inc. San Francisco, CA, USA). To stain nuclei, cells were incubated for 10 min at room temperature with 500 μg/ml propidium iodide (PI, Sigma-Aldrich, St Louis, Missouri, USA) or 0.2 μg/μl DAPI (Sigma-Aldrich, St Louis, Missouri, USA). Cell preparations were mounted on microscope slides with VectaShield (Vector Laboratories Inc. Burlingame, CA, USA) and visualized on a confocal laser scanning microscope (TCP-SP5, Leica Microsystems, Heidelberg, Germany) using a Plan Neo Fluor 63× (NA = 1.4) oil-immersion objective. Image analysis of digitized confocal microscopic files using the ImageJ 1.62 software to determine the nuclear to cytoplasmic ratio (Fn/c) were performed as previously [40,41].

2.5. Immunoprecipitation

Nuclear extracts (500 μg) were pre-cleared with recombinant protein G-agarose beads (Invitrogen, Carlsbab, CA, USA) for 2 h at 4 ºC; next, beads were removed by centrifugation at 1250 *g* for 5 min and pre-cleared extracts were incubated overnight at 4 ºC with the appropriate immunoprecipitating antibody. Parallel incubations with an irrelevant IgG0 antibody were performed. Thereafter, 10 μl of protein G-agarose beads were added and incubated overnight at 4 ºC. The immune complexes were collected by centrifugation at 1250 *g* for 5 min, washed three times for 5 min with 500 μl of wash buffer [50 mM Tris–HCl pH 8.0, 150 mM NaCl, 1 mM EDTA pH 8.0, 0.5% (v/v) Triton X-100, 0.05% (w/v) SDS and 1 mM PMSF], and eluted by boiling in 10 μl of Laemmli sample buffer [50 mM Tris–HCl pH 6.8, 2% (w/v) SDS, 10% (v/v) glycerol, 1% (v/v) 2-mercaptoethanol, 0.01% (w/v) bromophenol blue]. GFP fusion proteins were immunoprecipitated using the GFP-Trap® bead system (Chromotek, Germany) in accordance with the manufacturer's instructions.

2.6. Cell fractionation and Western blotting

Isolation of total, cytosolic and nuclear extracts were carried out as described [25]. Protein samples (80 μg) were electrophoresed on 10% SDS-polyacrylamide gels and transferred to nitrocellulose membranes (Hybond-N+, Amersham Pharmacia, GE Healthcare, Buckinghamshire, UK) by using a Transblot apparatus (Bio-Rad, Hercules, CA, USA). Membranes were blocked for 1–3 h in TBS-T [10 mM Tris-HCl pH 8.0, 150 mM NaCl, 0.05% (v/v) Tween-20] with 6–15% (w/v) low-fat dried milk. Next, membranes were incubated overnight at 4 °C with the appropriate primary antibody. After three washes in TBS-T, membranes were incubated with the corresponding horseradish peroxidase-conjugate secondary antibody (Amersham Pharmacia, GE Healthcare, Buckinghamshire, UK) and developed using the ECL Western blotting analysis system (Amersham Pharmacia, GE Healthcare, Buckinghamshire, UK).

2.7. Bacterial protein expression and purification

The ZZ domain of Dp71d was purified from bacteria as His6-tagged protein using nickel affinity chromatography under native conditions [42]. The IMP proteins were expressed and purified from bacteria as GST-fusion proteins under native conditions as described [35]. Proteins were then further purified by gel filtration using a HiPrep 26/60 Sephacryl S-200 High Resolution column attached to an ÄKTA Purifier system (GE Healthcare Company, Buckinghamshire, UK) and concentrated using Amicon centrifugal concentrators (Millipore Corporation, Billerica, MA, USA). Expression of GST and GST-Dp71d proteins was induced as described [22]. Protein concentrations were estimated by absorbance measurement at 280 nm and the theoretical molar extinction coefficient.

2.8. Biotinylation and ALPHAscreen assay

IMPα/IMPβ1 were biotinylated using the sulfo-NHS-biotin (sulfo-N-hydroxysuccinimide Biotin) reagent. Briefly, 3.5 mg of IMP was incubated with 250 μl of 10 mM sulfo-NHS-Biotin on ice for 2 h. Unbound biotin was removed using a PD-10 desalting column (GE Healthcare Company, Buckinghamshire, UK), and the resultant biotinylated IMPs were concentrated to between 100 and 250 μM in an Amicon-30 centrifugal concentrator.

Interaction between His6-tagged ZZ fusion protein and biotinylated-IMPs was assessed using an established ALPHAScreen assay (PerkinElmer, Wellesley, MA, USA) [43], whereby IMPs α2 and β1 were pre-dimerized at 13.6 μM for 15 min at room temperature in intracellular buffer (20 mM HEPES pH 7.4, 110 mM KCl, 5 mM $NaHCO_3$, 5 mM $MgCl_2$, 1 mM EGTA, 0.1 mM $CaCl_2$, 1 mM DTT) to generate the IMPα2/β1 heterodimer for binding studies. 384-well white Optiwell plates (PerkinElmer, Wellesley, MA, USA) were coated with 30 nM of His6-tagged ZZ fusion protein/well and incubated for 30 min with increasing IMP concentrations (0–60 nM). 1 μl of a 1:10 dilution of the nickel chelate acceptor beads and 1 μl of 2.5% (w/v) of BSA was subsequently added and the samples incubated at room temperature for 90 min. 1 μl of a 1:10 dilution of the streptavidin donor beads was then added and the samples were incubated at room temperature for a further 2 h. Protein binding was subsequently detected using a FusionAlpha plate reader (Perkin Elmer, Wellesley, MA, USA).

2.9. GST binding assays

5 μg of GST and GST–Dp71d proteins bound to glutathione-Sepharose beads was incubated overnight with 1 mg of total protein extract of C2C12 cells at 4 °C in interaction buffer [50 mM Tris–HCl pH 8′0, 150 mM NaCl, 1 mM PMSF, 1% (v/v) Triton X-100, 0.05% (w/v) SDS, 1× complete protease inhibitor cocktail (Roche Applied Science, Indianapolis, USA)]. Beads were recovered by centrifugation at 1000 *g* at 4 °C and washed three times in 1 ml of ice-cold Wash Buffer [50 mM Tris–HCl pH 7.5, 150 mM NaCl, 1 mM EDTA pH 8.0, 1 mM PMSF, 1% (v/v) Triton X-100]. Finally, proteins were eluted by adding 1 volume of 2× Laemmli buffer and heating at 95 °C, 5 min. Interacting proteins were identified by SDS-PAGE and Western analysis using the appropriate primary antibodies. For *in vitro* binding of Dp71d with emerin, full-length emerin was produced by *in vitro* transcription-translation of pSG5-Emerin plasmid using the TnT® Quick Coupled Transcription/Translation System in the presence of [^{35}S]methionine (Amersham Bioscience, GE Healthcare, Buckinghamshire, UK), according to the manufacturer's instructions (Promega, Madison, WI, USA). Affinity purified GST and GST–Dp71d proteins immobilised on glutathione-Sepharose beads (2.5 μg) were incubated with ^{35}S-Emerin overnight at 4 °C with agitation in binding buffer (140 mM K-acetate, 15 mM Hepes, pH 7.1, 1.5 mM EDTA, 5 mM $MgSO_4$). After overnight incubation, glutathione beads were washed extensively three times with binding buffer containing 0.5% (v/v) Triton X-100, eluted with Laemmli sample buffer and subjected to SDS-PAGE. Gels were imaged using the Typhoon trio (Amersham Bioscience, GE Healthcare, Buckinghamshire, UK).

2.10. DTAF labelling of His_6-ZZ

His_6-ZZ protein was expressed in bacteria, purified by Nickel-affinity chromatography, and fluorescently labelled with DTAF (5,-[4,6-dichlorotriazinyl]aminofluorescein). 500 μg His_6-ZZ was incubated with 0.4 mg/ml DTAF dissolved in 250 mM Bicine buffer (*N*,*N*-bis(2-hydroxyethyl)-glycine), pH 9.5, room temperature for 90 min. Unbound excess dye was removed using a PD-10 desalting buffer (Amersham Bioscience, GE Healthcare, Buckinghamshire, UK).

2.11. In vitro reconstitution of nuclear transport

Nuclear transport of fluorescently labelled His_6-ZZ (DTAF-ZZ) was reconstituted *in vitro* in mechanically perforated HTC cells as previously [44], with GFP-tagged SV40 large tumour antigen (GFP-T-ag) used as a control. Briefly, the plasma membrane was perforated mechanically, leaving the nuclear envelope intact. Perforated cells were then inverted on to a microscope slide, into 5 μl of nuclear transport mix, consisting of 45 mg/ml rabbit reticulocyte lysate (Promega, Madison, WI, USA), an ATP regenerating system (0.125 mg/ml creatine kinase, 30 mM creatine phosphate and 2 mM ATP), 70 kDa Texas Red-conjugated dextran (to monitor nuclear integrity), and 2 μM DTAF-ZZ or GFP-T-ag in IB buffer (intracellular buffer; 110 mM KCl, 5 mM $NaHCO_3$, 5 mM $MgCl_2$, 1 mM EGTA, 0.1 mM $CaCl_2$, 20 mM HEPES and 1 mM dithiothreitol, pH 7.4). The involvement of individual IMPs in Dp71d nuclear import was determined by preincubating reticulocyte lysate for 15 min at room temperature with inhibitory monoclonal antibodies to IMPα2 (Rch1), β1 or β3 (BD Biosciences, San Jose, CA, USA). To determine the extent to which binding to nuclear components contributes to nuclear accumulation, 0.025% CHAPS (3-[(3-cholamidopropyl) dimethylammonio]-1-propanesulfonic acid) was included to permeabilise the nuclear envelope (see [45,47]); only proteins able to bind to nuclear components are able to accumulate in the nucleus under these conditions.

3. Results

3.1. The ZZ domain is required for Dp71d nuclear import

Although nuclear localisation of Dp71d implies the existence of a facilitated nuclear import mechanism, the NLS responsible has not been identified. As a first step to address this, we subcloned full-length Dp71d or its N- and C-terminal halves into the Tetra-GFP reporter system (Fig. 1A), which encodes four in-frame fused copies of GFP [34], to generate GFP-tagged truncation derivatives of Dp71d larger than 45 kDa, the upper limit for free diffusion through the NPC. Analysis in transfected cells expressing the constructs by confocal fluorescence microscopy (CLSM) revealed that both full-length and the N-terminal portion of Dp71d (TetraGFP-Amino), containing the WW domain, EF-hands motifs and the ZZ domain, readily targeted TetraGFP to the nucleus, while the C-terminal half of Dp71d (TetraGFP-Carboxy), bearing the syntrophin-binding domain and leucine heptads motifs, was retained in the cytoplasm (Fig. 1B). Quantitative analysis of confocal images to determine the nuclear to cytoplasmic ratio (Fn/c) confirmed these observations, with TetraGFP-Dp71d and TetraGFP-Amino exhibiting Fn/c values of c. 0.7, significantly higher than that of TetraGFP alone (Fn/c of 0.44 (Fig. 1C)). It has previously been shown that the NLS of several zinc finger-containing proteins are localised to their zinc finger regions [48,52], and hence we generated two additional GFP-tagged constructs (Fig. 1A). Removal of the ZZ domain from the N-terminal construct resulted in reduced nuclear localisation of TetraGFP, suggesting that this domain is responsible for Dp71d nuclear localisation. Similarly, the ZZ domain alone appeared to be sufficient to target Tetra-GFP to the nucleus (Fig. 1B), Fn/c value of 2.0 (Fig. 1C), supporting the idea that the ZZ domain confers Dp71d nuclear localisation.

To determine the requirement for Zn^{2+}-binding on the nuclear translocation of Dp71d conferred by the ZZ domain, the effect of the zinc-chelating agent TPEN on endogenous Dp71d nuclear localisation was analysed. Strikingly, TPEN-treated cells exhibited a drastic reduction in nuclear staining for endogenous Dp71d, compared with control cells (Fig. 2A; Fn/c value of 0.5 compared to that of 1.6 in its absence — Fig. 2A right); similarly, the predominantly nuclear localisation of TetraGFP-ZZ was reduced by TPEN treatment (Fig. 2B; Fn/c value of 1.8 compared to c. 3 in its absence — Fig. 2B right). This was also confirmed using subcellular fractionation approaches, with analysis of total, cytosolic and nuclear extracts from C2C12 cells revealing that although the total levels of Dp71d

remain virtually unaltered in TPEN-treated cells, there is a significant decrease ($p = 0.0084$) in the level of Dp71d in the nucleus upon TPEN treatment (Fig. 2C, left; n/c ratio of c. 1 in the presence of TPEN compared to 1.6 in its absence, Fig. 2C right). TPEN had no effect on the subcellular distribution of β-dystroglycan, a protein that lacks a zinc finger but localises in the nucleus in NLS/IMP-dependent fashion [40], as indicated by immunofluorescence/CLSM (Supp. Fig. 1A) as well as subcellular fractionation/Western analysis (Supp. Fig. 1B), confirming the specificity of the effect of TPEN on Dp71d, as a zinc finger-containing protein.

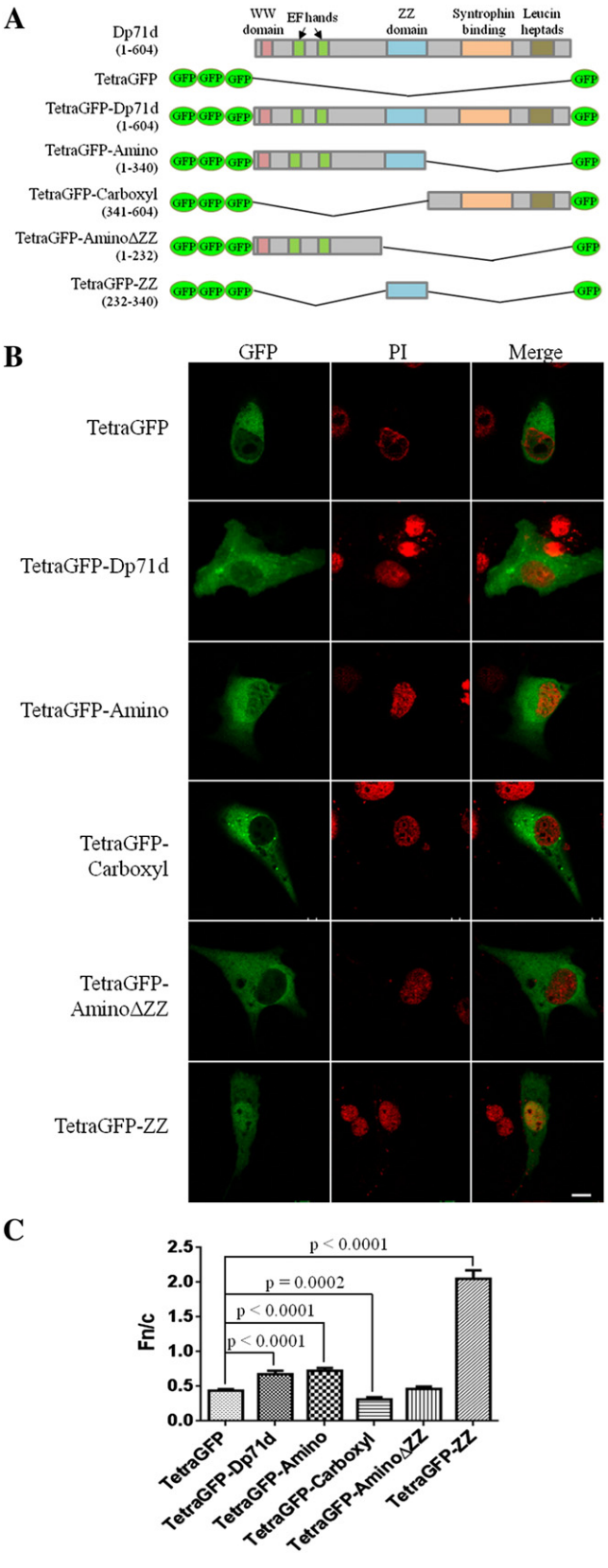

The effect of single alanine substitutions of key residues within the dual Zn^{2+}-fingers of Dp71d (see also [53]), or combinations thereof was tested for the effect on subcellular localization (the schematic in Fig. 3 indicates the site of the mutations). Substitution of single histidine residues in the first (ZZ-1) and second (ZZ-3) Zn^{2+}-fingers, as well as substitution of the third cysteine in the first Zn^{2+}-finger (ZZ-2) did not reduce the prominent nuclear localisation of the TetraGFP-ZZ fusion protein (Fn/c values of 2 or above in all cases, including wild type; Fig. 3 bottom). The ZZ-3 substitution, in fact, increased the extent of nuclear accumulation (Fn/c of c. 5), presumably as a result of an unmasking effect (see [54]) with respect to other residues within the Zn^{2+}-finger region of Dp71d that may contribute to Dp71d nuclear localization. In contrast, substitution of the second cysteine in the second Zn^{2+}-finger (ZZ-4), markedly reduced nuclear localisation of TetraGFP-ZZ (Fn/c of 0.6; Fig. 3 bottom), consistent with the idea that specific amino acid residues within the Zn^{2+}-fingers play a critical role in Dp71d nuclear import. A combination of the ZZ-2 and enhancing ZZ-3 substitutions (ZZ-5) also resulted in reduced nuclear accumulation (Fn/c of 1.3), indicating that the Dp71d NLS is complex, and dependent not only on the Zn^{2+}-fingers themselves, but potentially also on other residues within the Zn^{2+}-finger domain (see above; [48,50,55]).

3.2. Nuclear import of Dp71d is dependent on nuclear pore proteins and Ran

To assess whether ZZ-mediated nuclear translocation of Dp71d is dependent on a conventional IMP-dependent pathway, we first examined whether the effect of *A. bisporus* lectin (ABL), which targets the *N-acetyl* glucosamine sugar moiety within many of the nucleoporins that make up the NPC, hence perturbing NPC-dependent nuclear transport [56], can alter the subcellular distribution of Dp71d. We found that ABL could indeed inhibit nuclear accumulation of endogenous Dp71d in C2C12 cells (Fig. 4A), resulting in a predominantly cytoplasmic localisation in contrast to the nuclear localisation observed in its absence (Fn/c values of 0.7 compared to 1.3 respectively; Fig. 4A below). Similarly, nuclear accumulation of the TetraGFP-ZZ domain was reduced in ABL-treated cells (Fig. 4B), resulting in a Fn/c of 0.9 compared to that of 2.8 in its absence (Fig. 4B bottom). Similar results to those for Dp71d and TetraGFP-ZZ were observed for IMP-dependent nuclear accumulation of β-dystroglycan (see above [41]), but no effect was observed for GFP, a protein that passively enters the nucleus (Supp. Fig. S2AB), underlining the specificity of the effects. The results are thus consistent with the idea that Dp71d accesses the nucleus *via* the NPC, dependent on nucleoporin function.

Conventional IMP-dependent nuclear import through the NPC is dependent on the guanine nucleotide binding protein/GTPase Ran, which affects disassembly of IMP-cargo complexes [57,58]; to test the dependence of Dp71d nuclear accumulation on Ran, a RanQ69L dominant-negative mutant was used that is locked in the GTP-bound conformation and thus able to inhibit IMP-dependent nuclear protein

Fig. 1. The ZZ domain is necessary and sufficient for Dp71d nuclear localisation. (A) Schematic representation of Dp71d and its truncated derivatives fused to the TetraGFP reporter protein. The numbers on the left indicate the corresponding amino acid residues of Dp71d encoded by the fragments in each reporter construct. (B) C2C12 cells cultured on glass coverslips were transiently transfected with the indicated constructs, fixed 24 h post-transfection and stained with propidium iodide (PI) to enable visualization of nuclei. Cells were imaged by CLSM, with typical single Z-sections shown (scale bar is 10 μm). (C) Quantitative analysis for the nuclear to cytoplasmic ratio (Fn/c) of the reporter proteins was performed using the ImageJ software, as described in Section 2. Results represent the mean +/− SEM ($n > 50$) from a series of three separate experiments. Significant differences between TetraGFP and full-length Dp71d and its truncated derivatives are denoted by the p values (Student's *t*-test).

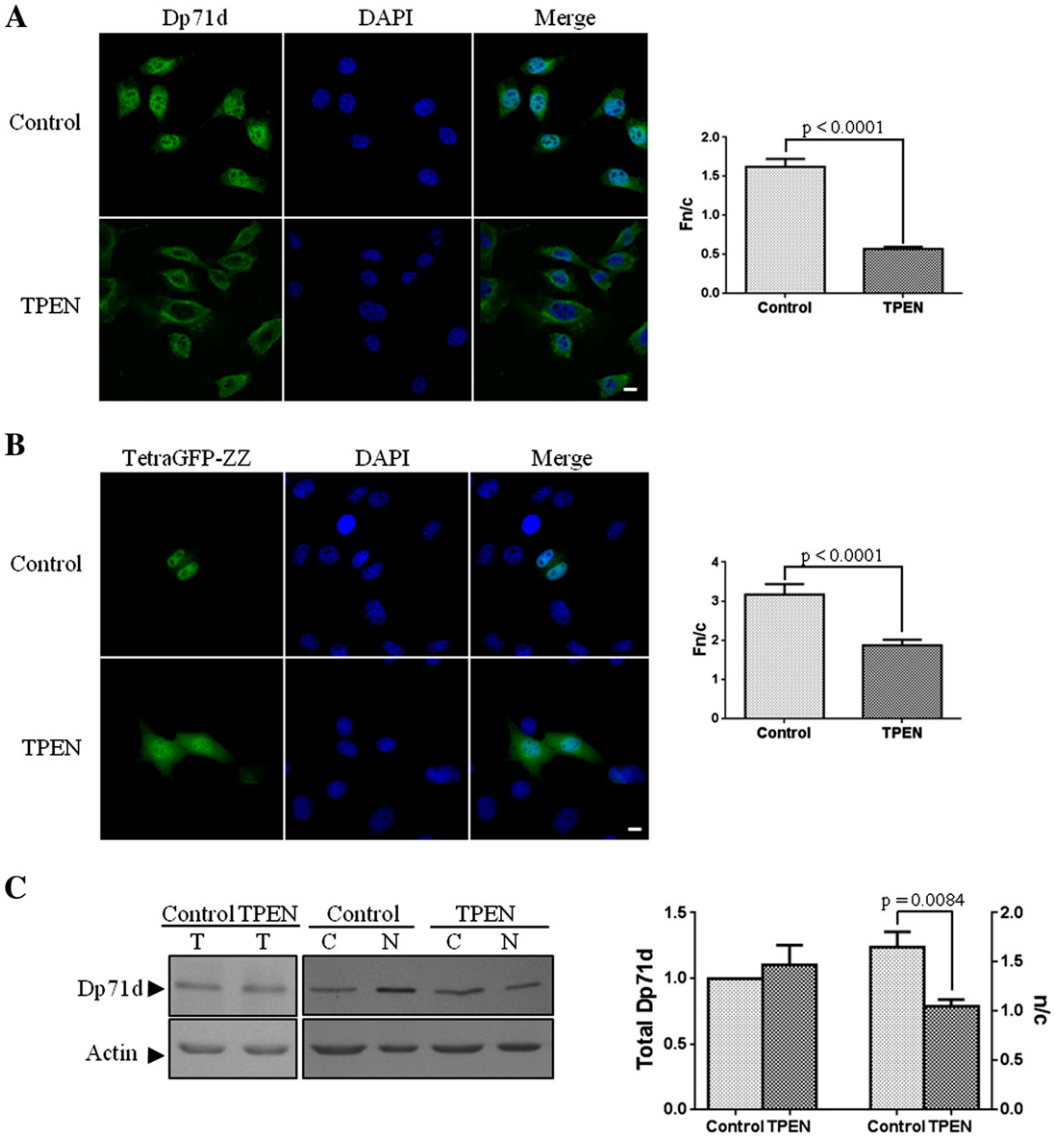

Fig. 2. The Zn^{2+}-chelating agent TPEN reduces nuclear localisation of Dp71d. (A) C2C12 cells seeded on glass coverslips were incubated for 24 h with 1.1 μM TPEN in DMSO or DMSO alone (control), prior to fixation, immunolabelling with anti-Dp71 antibody (green) and counterstaining with DAPI to enable nuclei to be visualized (blue). (B) C2C12 cells cultured on glass coverslips were transiently transfected with TetraGFP-ZZ construct and treated with TPEN 8 h later as described above, prior to fixation and staining with DAPI. Scale bar 10 μm. In both cases, confocal images such as those shown were subjected to image analysis as described in the legend to Fig. 1 for endogenous Dp71d (A) or TetraGFP-ZZ (B). Results represent the mean +/− SEM ($n > 50$) from a series of three separate experiments, with significant differences between control and TPEN-treated cells denoted by the p values. C) Cells were treated without or with TPEN as above, and then total (T) cytoplasmic (C) and nuclear (N) extracts prepared as described in Section 2, were subjected to SDS-PAGE/Western blot analysis employing a specific anti-Dp71d antibody. Membranes were stripped and reprobed for actin as loading control (left panel). Densitometric analysis of immunoblot autoradiograms was performed to determine both the total level and the nuclear/cytoplasmic ratio (n/c) of Dp71d in control and TPEN-treated cells (right panel), relative to untreated cells. Results represent the mean +/− SEM for 3 separate experiments, with significant differences between control and TPEN-treated cells denoted by the p values.

import [37]. C2C12 cells were cotransfected to express TetraGFP-ZZ and dsRed-tagged RanQ69L, confocal microscopic analysis showing that TetraGFP-ZZ shifted from the nucleus to the cytoplasm in the presence of dsRed-RanQ69L (Fig. 4C), with quantitative analysis confirming this observation (right panel). Ran is thus clearly implicated as playing a role in the nuclear import of Dp71d.

3.3. Nuclear import of Dp71d is dependent on IMPα/β1

To confirm the nuclear import ability of the ZZ of Dp71d, we firstly used an *in vitro* reconstituted nuclear transport system based on mechanically perforated HTC cells as previously [44,47,59]. Fluorescently labelled bacterially expressed His-tagged ZZ (DTAF-ZZ) was able to accumulate rapidly and strongly in the nucleus ($Fn/c_{max} \approx 7$, $t_{1/2} \approx 4.5$ min, Fig. 5AB, and data not shown), to an extent greater than a well-characterised Simian Virus SV40 large tumour antigen (T-ag) NLS-containing GFP fusion protein ($Fn/c_{max} \approx 2$; data not shown), supporting the idea that ZZ accumulates efficiently in the nucleus. To examine the nuclear import mechanism of Dp71d in more detail, we added antibodies specific for different IMPs in the nuclear transport assay as previously [40,41,55,56]; antibodies to both IMPα2 and IMPβ1, but not IMPβ3 significantly ($p < 0.015$) reduced (c. 50%) nuclear accumulation of DTAF-ZZ (Fig. 5AB; see Fig. 5C for pooled data), implying that Dp71d nuclear import is strongly dependent on IMPα2/β1 and not other IMPs. To assess the extent to which nuclear accumulation of Dp71d is dependent on nuclear retention through binding to nuclear components in addition to active, IMP-dependent transport, experiments were performed in the presence of the nuclear envelope

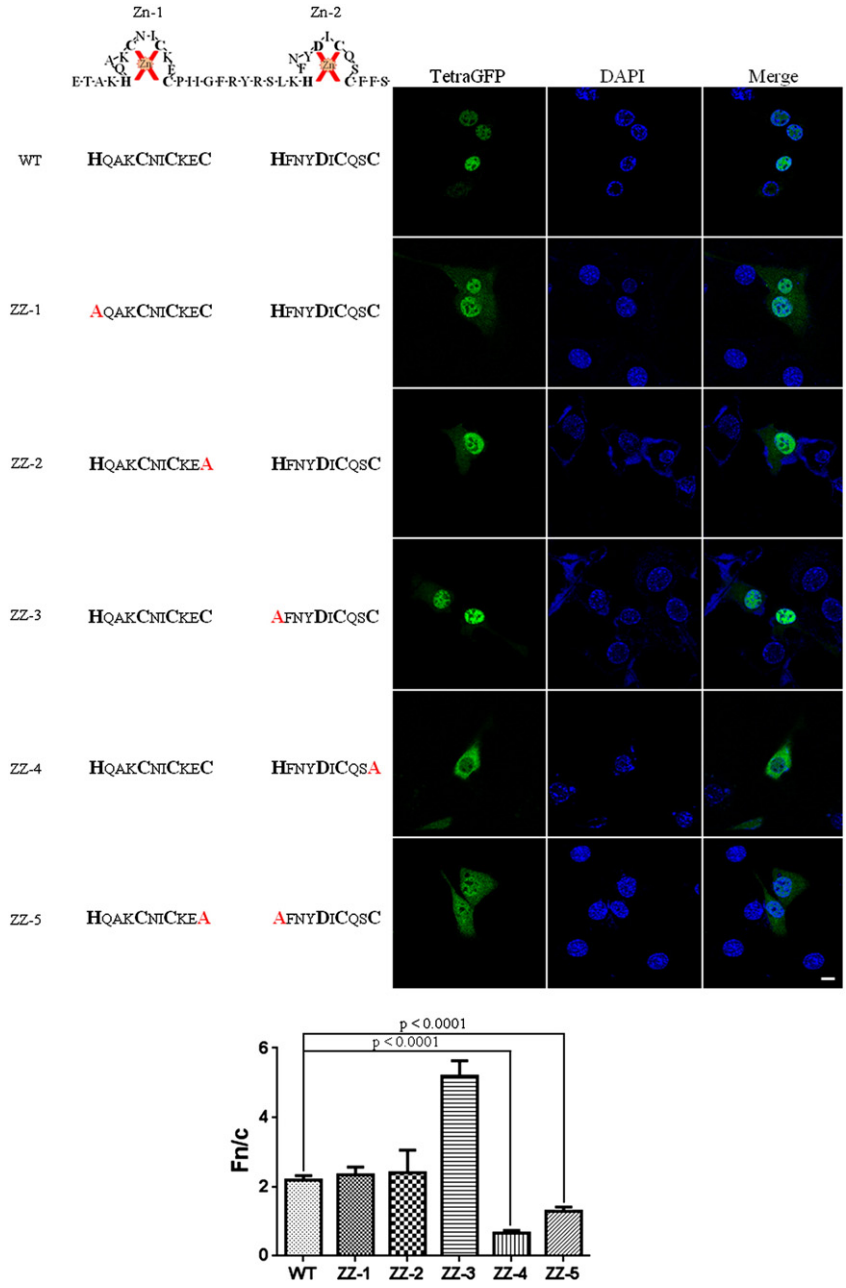

Fig. 3. Identification of key Zn^{2+}-chelating residues conferring Dp71d nuclear translocation. C2C12 cells cultured on coverslips were transiently transfected to express TetraGFP-ZZ (WT) or mutant derivatives thereof (ZZ-1 to ZZ-5). Cells were fixed, stained with DAPI, and then subjected to CLSM analysis; typical single Z-sections are shown (scale bar is 10 μm). A schematic representation of the zinc finger motifs (Zn-1 and Zn-2) of the ZZ domain of Dp71d is shown (see also [53]), highlighting the amino acid substitutions analysed; potential Zn^{2+}-chelating amino acids are shown in bold and mutated residues denoted in red. Quantitative analysis of the levels of nuclear accumulation (Fn/c ratio) of each ZZ derivative mutant was performed and compared with that of WT, as per the legend to Fig. 1. Results represent the mean +/− SEM for three separate experiments (n = 50), with significant differences between mutant and WT constructs denoted by the p values.

permeabilising detergent CHAPS (Fig. 5D,E). In the presence of CHAPS, the level of DTAF-ZZ accumulation fell markedly (Fn/c_{max} of c. 2.5), in essentially comparable fashion to the effect on T-ag ($Fn/c_{max} \approx 1$), which is unable to bind to nuclear components. That nuclear accumulation of DTAF-ZZ was not completely abolished in the presence of CHAPS, however, indicates that it retains an ability to bind to nuclear components, presumably through its Zn^{2+}-finger domain, but facilitated, IMP-dependent nuclear import is clearly mainly responsible for its nuclear accumulation.

To confirm that full length Dp71d can interact with IMPs in a physiological context, pull-down assays were initially performed (Fig. 6A), whereby recombinant, bacterially expressed GST and GST-Dp71d proteins were immobilised on sepharose, prior to incubation with lysates from C2C12s and subsequent Western blot analysis. Both IMPα2 and β1 were found to bind efficiently to GST-Dp71d but not to GST alone, implying the specificity of the interaction with IMPα2/β1. Thus, full length Dp71d can interact with IMPα2/β1. Consistent with this idea, immunoprecipitation from intact cells indicated that IMPα2 and IMPβ1 but not IMPβ2, interacted with the ZZ domain expressed as a TetraGFP-fusion in transfected cells, but not with TetraGFP alone, illustrating the specificity of the interaction between the ZZ domain of Dp71d and IMPα2/β1 (Fig. 6B). Importantly, IMPα2 and β1 binding was abolished in the ZZ-4 mutant, which is also impaired in nuclear localisation, but not in the nonaffected mutant ZZ-1 (see Fig. 3), which

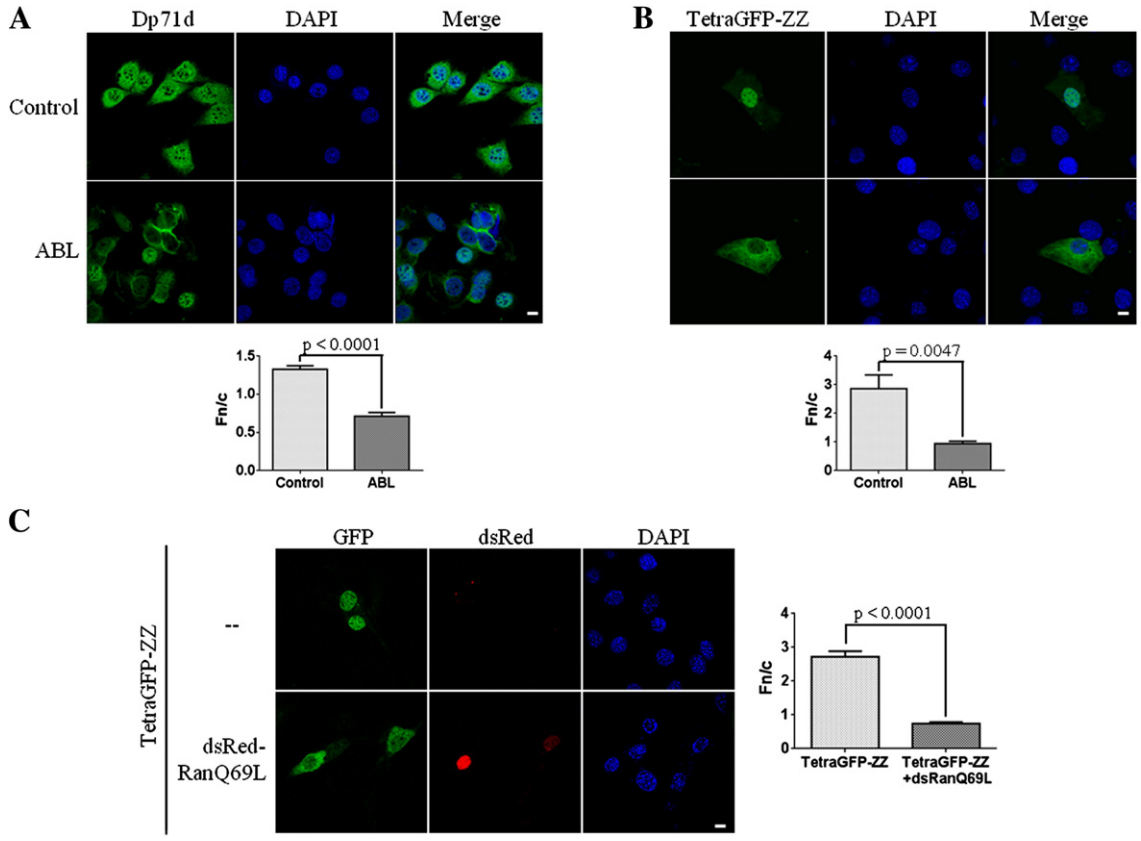

Fig. 4. Dp71d nuclear accumulation occurs through the NPC and is dependent on Ran. (A) C2C12 cells seeded on glass coverslips were treated for 24 h with the *Agaricus bisporus* lectin (ABL) diluted in PBS or with PBS alone (Control), prior to fixation, immunostaining using anti-Dp71d primary and fluorescein-coupled secondary (green) antibodies and counterstained with DAPI (nuclei, blue). (B) C2C12 cells cultured on coverslips were transiently transfected with vector expressing TetraGFP-ZZ fusion protein (green) and 8 h post-transfection were treated with ABL as described above, and subsequently fixed and stained with DAPI (nuclei, blue). (C) C2C12 cells seeded on glass coverslips were cotransfected to express TetraGFP fused to the ZZ domain of Dp71d (green) with or without (−) the dominant negative Ran derivative dsRed-RanQ69L (red). Cells were fixed 24 h post-transfection and stained with DAPI (nuclei, blue). Samples from Panels A, B and C were imaged by CLSM and analysed as per the legend to Fig. 1 (scale bars are 10 μm). Results represent the mean +/− SEM for 3 separate experiments (n = 50), with significant differences between control and ABL-treated cells (A and B) or RanQ69L-expressing cells (C) denoted by the p values.

clearly implying that the NLS within the ZZ domain, mutated in ZZ-4, is the target for IMPα2/β1 binding, and that IMPα2/β1 is the nuclear transporter for Dp71d in living cells.

Finally, to confirm that IMP binding to Dp71d was direct, binding of recombinant, bacterially expressed ZZ fused to His-tagged GFP to IMPs was tested in an ALPHAScreen binding assay [43,44], with His-tagged GFP alone as a control. The ZZ was able to be recognised by GST-IMPα2 and GST-IMPβ1, but not GST alone (Fig. 6C). Significantly, the IMPα2/β1 heterodimer bound with very high binding affinity (apparent dissociation coefficient of c. 0.25 nM, compared to an over 10 times higher value for IMPα2 or β1 alone), implying that, consistent with the results from Fig. 5A,B, IMPα2/β1 is likely the major nuclear transporter for Dp71d through the high affinity of the direct interaction.

3.4. Dp71d can shuttle between the nucleus and cytoplasm

Since Dp71d is distributed in both the cytoplasm and the nucleus, with its subcellular localisation modulated by specific stimuli [30], it is likely that Dp71d may be a nucleocytoplasmic shuttling protein, with a functional nuclear export pathway in addition to its IMPα2/β1-dependent nuclear import pathway clearly implicated above. To assess whether Dp71d possesses an exportin-1/CRM1-recognised nuclear export pathway, the effect on the subcellular distribution of endogenous and ectopically expressed Dp71d of the CRM1-specific inhibitor leptomycin B (LMB) was tested (Fig. 7A–D). Effectiveness of LMB treatment was confirmed using the NES-containing fusion protein constructs Rev-NES-GFP and its NES mutated variant Rev-NESmut-GFP, as positive and negative control respectively. As expected, localization of Rev-NES-GFP shifted from the cytoplasm to the nucleus in C2C12 cells upon LMB treatment, while Rev-NESmut-GFP did not respond to LMB and still localised to the cytoplasm, confirming that CRM1-mediated nuclear export was effectively blocked (see Supp. Fig. S3AB). We observed increased nuclear localization of endogenous Dp71d upon LMB treatment, which was supported by quantitative analysis (Fig. 7A). Similarly, ectopically expressed GFP-Dp71d accumulated in the nucleus to a significantly ($p < 0.0001$) greater extent in LMB-treated cells than in control cells (Fn/c of 2.8 and 0.6 respectively; Fig. 7B right). These results indicate that Dp71d indeed possess a CRM1-dependent NES. CRM1-recognised NESs generally include 4 or more closely spaced hydrophobic residues, often leucines; we identified five potential NES-like sequences within Dp71d, four within the N-terminal half and one in the C-terminal portion (see schematics in Fig. 7C,D, where the putative NES sequences are shown in the context of the constructs encoding the N- and C-terminal halves of Dp71d). In an initial attempt to determine the functionality of these NESs, we tested the effect of LMB on the subcellular distribution of TetraGFP-Amino and TetraGFP-ZZCarboxyl proteins in C2C12 cells. We found that TetraGFP-ZZCarboxyl (Fig. 7D), but not TetraGFP-Amino (Fig. 7C) clearly relocalised from the cytoplasm to the nucleus upon LMB treatment, resulting in over 4-fold higher levels of nuclear accumulation (Fn/c of c. 2 compared to 0.4 in the absence of LMB; Fig. 7D right), implying that the C-terminus of Dp71d contains a functional CRM1-recognised NES, likely to comprise amino acids 505–515.

To confirm that Dp71d can associate with CRM1 in intact cells, we performed immunoprecipitation assays using a GFP-Trap approach. Consistent with the IF data, TetraGFP fused to full-length Dp71d or TetraGFP-ZZCarboxyl but not TetraGFP alone or TetraGFP-Amino

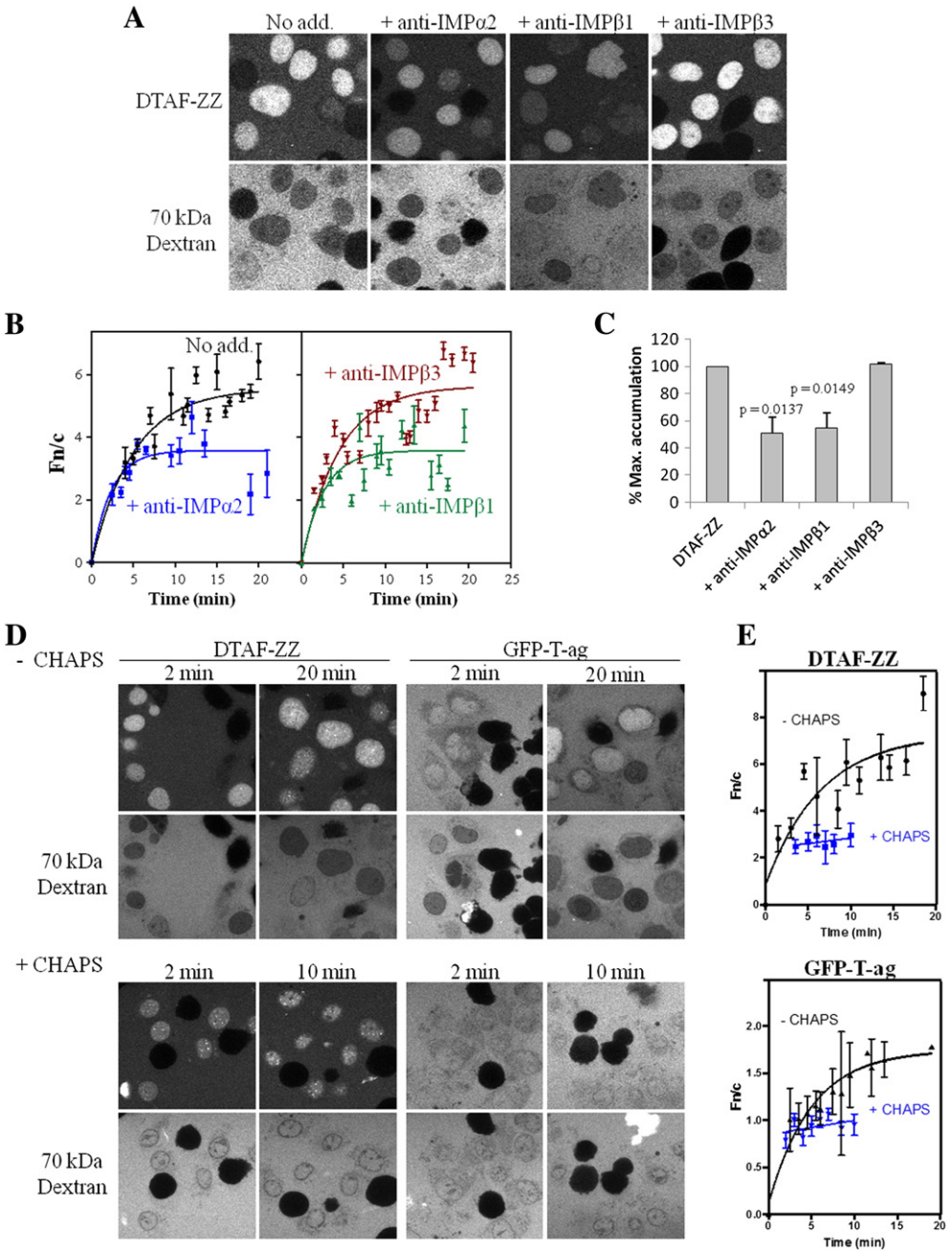

Fig. 5. Reconstitution of Dp71d nuclear accumulation *in vitro*; dependence on IMPα2 and IMPβ1. Nuclear import of DTAF-labelled ZZ domain of Dp71d was reconstituted *in vitro* in mechanically perforated HTC cells in the presence of exogenous cytosol (45 mg/ml rabbit reticulocyte lysate) and an ATP regeneration system as described in Materials and methods. (A) CLSM images were acquired periodically for accumulation of DTAF-ZZ (upper panels) into intact nuclei in the absence (No add.) or presence (45 μg/ml) of specific monoclonal antibodies to IMPα2, β1 or β3 (BD Biosciences, Franklin Lakes, New Jersey, USA) as indicated, which were pre-incubated with reticulocyte lysate for 15 min at room temperature prior to addition to the sample well. Nuclear integrity was monitored by exclusion of a Texas Red-labelled 70 kDa dextran (lower panels). (B) Image analysis performed on CLSM images such as those in (A) using ImageJ (NIH) software to determine the nuclear to cytoplasmic fluorescence ratio (Fn/c), calculated using the equation $Fn/c = (Fn - Fb) / (Fc - Fb)$, where Fn, Fb and Fc represent the nuclear, background and cytoplasmic fluorescence values respectively. Nuclear import kinetics were plotted using GraphPad Prism and exponential curves fitted. Each point represents the mean ± SEM, n > 10. (C) The % maximal accumulation (relative to No add.) was calculated from curves such as those in (B). Results represent mean ± SEM, n = 3. (D) CLSM images were acquired periodically for accumulation of DTAF–ZZ (left panels) and the control protein GFP-T-ag (right panels) into intact nuclei as per (A), in the absence (upper panels) or presence (lower panels) of 0.025% CHAPS to permeabilise the nuclear membrane, indicated by the lack of exclusion of a 70 kDa dextran (lower panels in each block). (E) Image analysis performed as per (B) on CLSM images such as those in (D). Each point represents the mean ± SEM, n > 10. Note that since steady state is reached within minutes in the absence of an intact nuclear membrane, data for CHAPS-treated samples are only presented for the first 10 min.

immunoprecipitated endogenous CRM1 from C2C12 cell lysates (Fig. 7E). To characterize the NES within Dp71d amino acids 505–515, we used site-directed mutagenesis to introduce alanine-substitutions of leucines 509, 512, and 515 in the context of full-length Dp71d sequence, and assessed the effect on subcellular localisation. Strikingly, in strong contrast to the predominantly cytoplasmic localisation of GFP-Dp71d, the NES mutant variant displayed significantly ($p < 0.0001$) greater nuclear accumulation, with an Fn/c > 1 (Fig. 7F). The clear implication was that Dp71d retains a CRM1 recognised NES within amino acids 505–515 that, together with an NLS in the ZZ-domain, confers the ability to shuttle in signal-dependent fashion between the nucleus and cytoplasm.

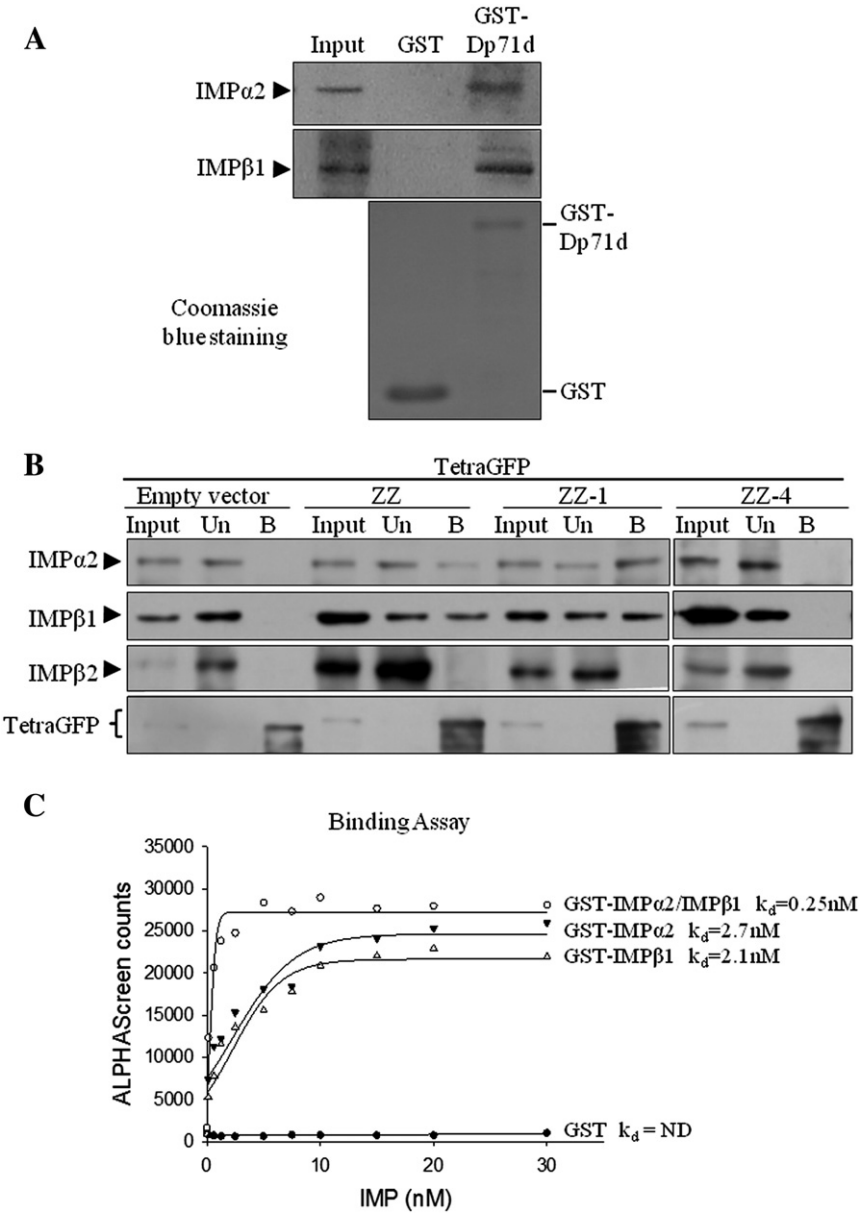

Fig. 6. Dp71d interacts with IMPα2/IMPβ1. (A) Pull down assays were performed by incubating glutathione-sepharose beads preincubated with bacterially expressed GST (negative control) or GST-Dp71d (full length) with nuclear extracts from C2C12 cells. Beads were recovered by centrifugation and eluted proteins were analysed by Western blot using specific antibodies against IMPα2 and IMPβ1 (upper panel). Inputs correspond to 5% of nuclear extract prior to pull down. Lower panel shows purified GST and GST-Dp71d proteins that were visualized by SDS-PAGE followed by Coomassie brilliant blue staining. (B) Complexation of the ZZ domain with IMPs in living cells. C2C12 cells transiently expressing TetraGFP or TetraGFP-ZZ proteins were immunoprecipitated using GFP-trap and immunoprecipitated proteins subjected to Western blot analysis using the indicated anti-IMP antibodies. Inputs correspond to 5% of nuclear extract prior to immunoprecipitation. Un, unbound fraction; B, bound fraction. (C) ALPHAScreen binding assays [43] were performed by incubating the His-tagged ZZ domain of Dp71d with increasing concentrations (0–30 nM) of bacterially expressed GST alone or GST-IMPβ1, -IMPα2, or predimerized GST-IMPα2/β1 (where GST-IMPβ1 was biotinylated and GST-IMPα2 unlabelled) — see Section 2. Triplicate data points from a single typical experiment are representative of three independent experiments fitted using SigmaPlot software to determine the apparent dissociation constants (K_d). ND, not able to be determined due to low binding.

3.5. Nuclear translocation of Dp71d is dependent on microtubule integrity and dynein

Since Dp71d is cytoskeleton-associated, we examined whether the cytoskeleton plays a role in Dp71d nuclear translocation in comparable fashion to a number of other proteins of interest [60,61]. C2C12 cells were treated with the actin-depolymerizing agent cytochalasin B or the microtubule-depolymerizing agent nocodazole, fixed, stained with phalloidin or anti-α-tubulin antibody respectively (Fig. 8A), as well as with a specific antibody to Dp71d (Fig. 8B). No significant changes were observed in the subcellular distribution of Dp71d after cytochalasin B treatment, suggesting that actin filaments do not play a substantial role in Dp71d nuclear localisation (Fig. 8B; top panels, with Fn/c values of around 1 in both control and treated cells, right). In stark contrast, nocodazole treatment significantly ($p < 0.0001$) decreased the extent of nuclear accumulation of endogenous Dp71d (Fn/c of 0.6), compared with control cells (Fig. 8B bottom panels). Subcellular fractionation/Western analysis confirmed this (Fig. 8C), with quantitative analysis indicating that nuclear levels of Dp71d but not its total levels were significantly ($p < 0.0001$) decreased (~45%) compared to control cells (Fig. 8C, right), consistent with the idea that efficient Dp71d nuclear accumulation is dependent on microtubule integrity.

To test the role of the microtubule motor protein dynein, involved in retrograde transport towards the nucleus of a number of proteins [62,64], in Dp71d nuclear translocation, C2C12 cells were treated with erythro-9-(2-hydroxy-3-nonyl)adenine (EHNA), an inhibitor of dynein

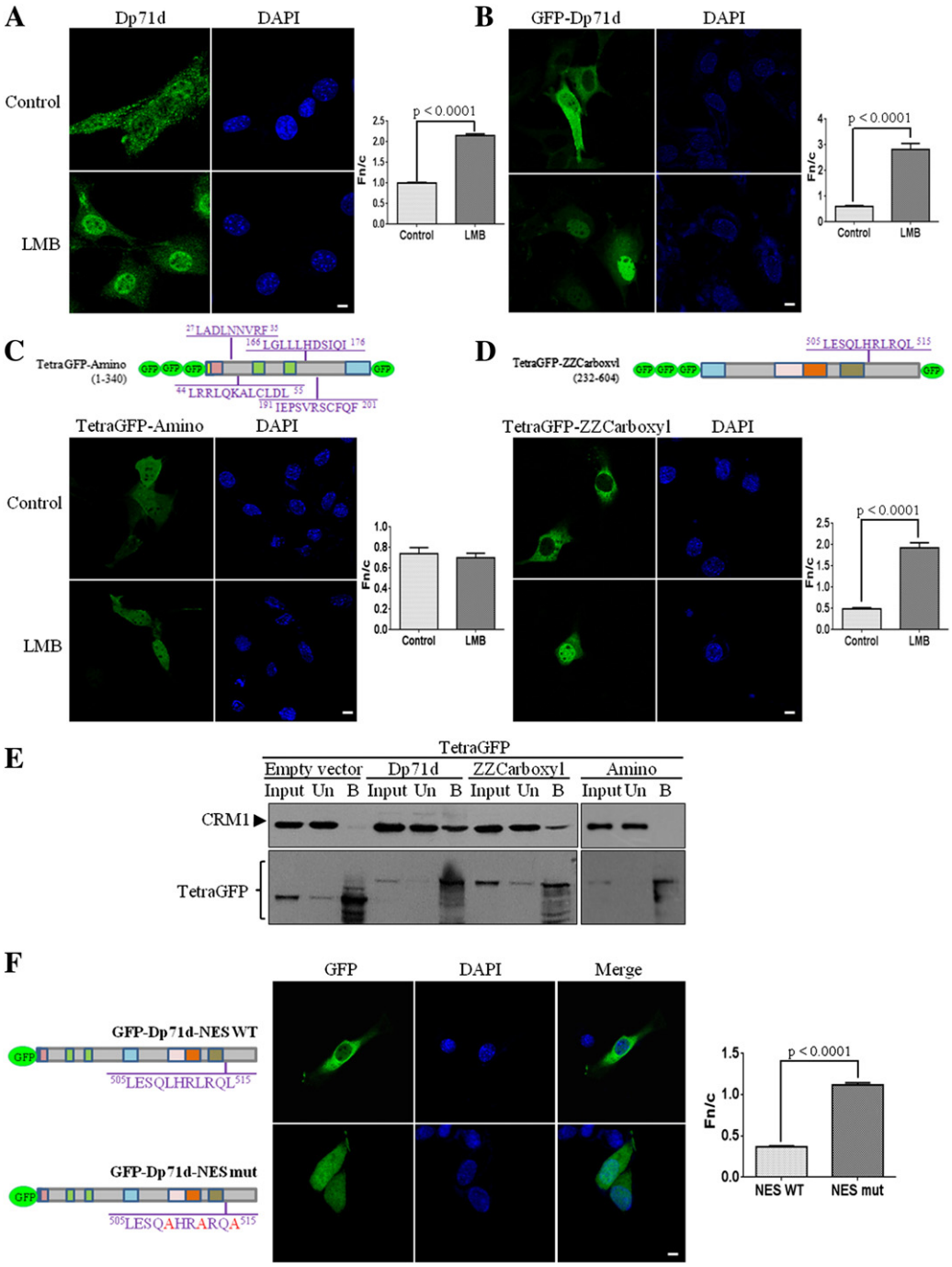

Fig. 7. Identification of a CRM1-recognised nuclear export signal (NES) in the carboxy-terminal domain of Dp71d. (A) C2C12 cells seeded on glass coverslips were incubated for 24 h with the CRM1-specific inhibitor Leptomycin B (LMB) diluted in methanol or with methanol alone (control). Cells were immunostained with primary anti-Dp71d antibody and a fluorescein-conjugated secondary antibody (green) and counterstained with DAPI (nuclei, blue). (B–D) C2C12 cells seeded on glass coverslips were transfected to express GFP-Dp71d, TetraGFP-Amino or TetraGFP-ZZCarboxyl (green) and 8 h post-transfection incubated for additional 12 h without (control) or with LMB. Schematics of the N- and C-terminal portions of Dp71d expressed in the TetraGFP-Amino and TetraGFP-ZZCarboxyl constructs respectively. The putative CRM1-recognised NES sequences located in each portion of Dp71d are shown. Cells were fixed, counterstained with DAPI (nuclei, blue), imaged by CLSM, and images such as those shown were analysed as per the legend to Fig. 1 for endogenous Dp71d (A) and GFP-based fusion proteins (B–D), as described in Section 2. Results represent the mean +/− SEM (n = 50), with significant differences in the absence or presence of LMB denoted by the p values. (E) Interaction between the C-terminal domain of Dp71d and CRM1 as determined by immunoprecipitation. Lysates from C2C12 cells transiently transfected to express TetraGFP, TetraGFP-Dp71d, TetraGFP-Amino or TetraGFP-ZZCarboxyl were immunoprecipitated using GFP-Trap and immunoprecipitated proteins subjected to Western analysis with antibodies against CRM1 and GFP. Inputs correspond to 5% of nuclear extract prior to immunoprecipitation; Un, unbound proteins; B, bound proteins. (F) C2C12 cells transiently transfected to express GFP fused to full-length Dp71d (GFP-Dp71d-NES WT; NES sequence within amino acids 505–515 is shown) or its mutant variant (GFP-Dp71d-NES mut; mutated residues within the NES are denoted in red) (green) were cultured on glass coverslips, fixed 24 h post-transfection, stained with DAPI (nuclei, blue) and subjected to CLSM analysis; typical single optical Z-sections are shown (scale bar, 10 μm). Fn/c values were determined as above, with significant differences between cells expressing WT or Mut NES denoted by the p values.

activity. In parallel, cells were treated with aurintricarboxylic acid (AA) an inhibitor of the anterograde microtubule motor kinesin, and the effect on subcellular distribution of Dp71d analysed by immunofluorescence/CLSM. In contrast to cells treated with AA (Fig. 9A), those treated with EHNA displayed reduced nuclear staining (Fig. 9B), with quantitative analysis indicating a significant ($p < 0.0001$) 30% reduction in

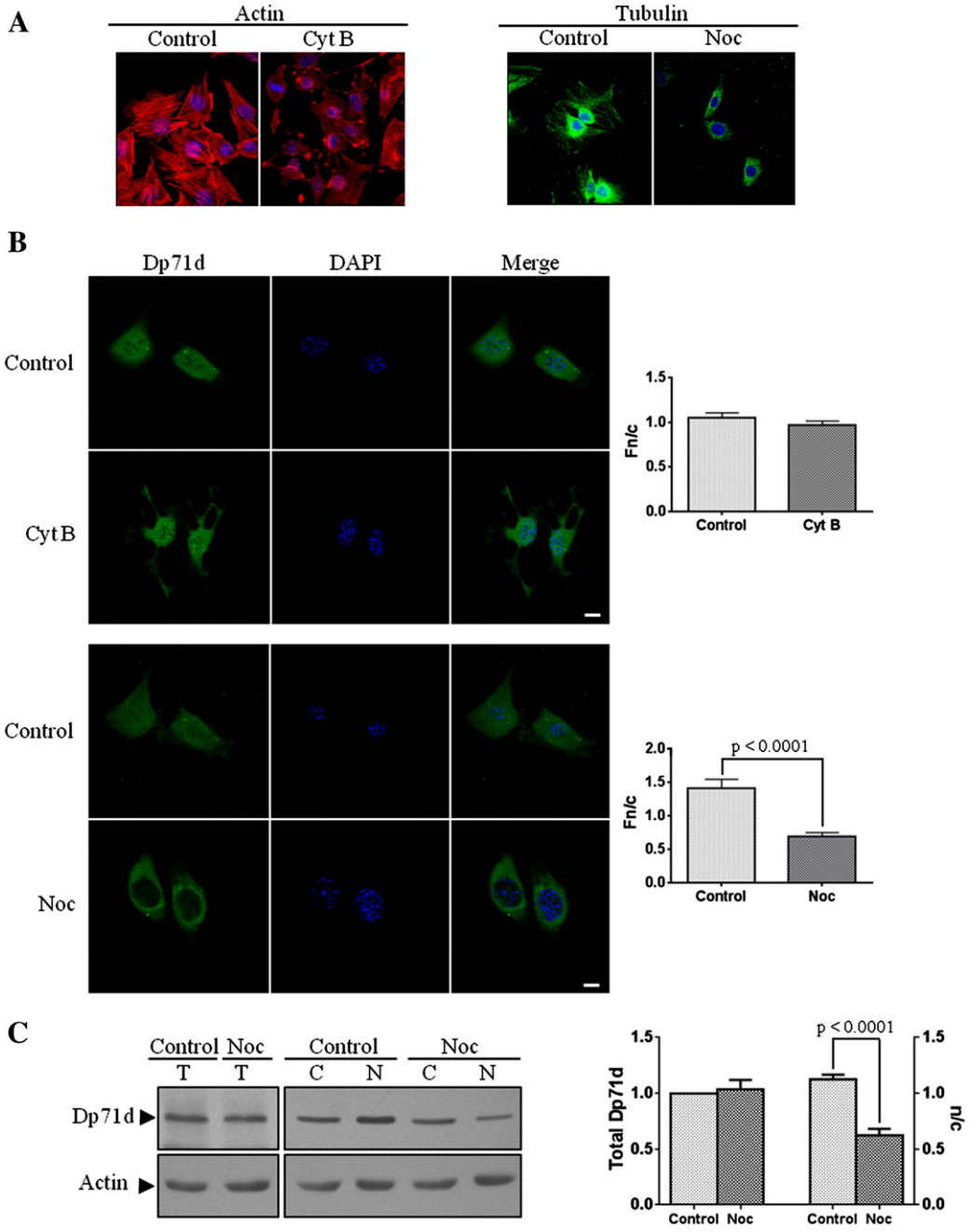

Fig. 8. Disruption of microtubule network impairs Dp71d nuclear localisation. C2C12 cells seeded in glass coverslips were treated for 4 h with cytochalasin B (Cyt B) or 5 h with nocodazole (Noc), diluted in DMSO, or with DMSO alone (control). (A) Cells were fixed and stained with phalloidin or with an anti-tubulin antibody in order to visualize effects on the actin-based cytoskeleton and microtubule network, respectively. (B) Cells treated as per (A) were immunolabelled with anti-Dp71d antibody and fluorescein-conjugated secondary antibody (green) and counterstaining with DAPI (nuclei, blue). Samples were imaged by CLSM (single optical Z-sections are shown; scale bar 10 μm), and image analysed as described in the legend to Fig. 1. Results represent the mean +/− SEM for 3 separate experiments (n = 50), with significant differences between control and Noc-treated cells determined by Student *t*-test. (C) Total (T), cytoplasmic (C) and nuclear (N) extracts obtained from control and Noc-treated cells were separated by SDS-PAGE and subjected to Western blot analysis for Dp71d. Membranes were stripped and reproved with anti-actin antibody to normalize for loading (left panel). Densitometric analysis of the immunoblots was performed as per the legend to Fig. 2C to determine both the total levels and the nuclear/cytoplasmic ratio (n/c) of Dp71d in control and nocodazole-treated cells (right panel). Results represent the mean +/− SD for 3 separate experiments, with significant differences between control and Noc-treated cells denoted by the p values.

the Fn/c value compared to untreated cells (Fig. 9B right). That the effects were specific was implied by the fact that none of the treatments altered subcellular distribution of β-dystroglycan (Supp. Fig. S4), a control cytoskeleton-associated protein whose nuclear translocation is mediated by IMPs. Thus, Dp71d nuclear import appears to be dependent on dynein, which is presumably the basis of the requirement for microtubule integrity for optimal nuclear accumulation efficiency; kinesin does not appear to be involved in Dp71d nuclear localization.

3.6. Physiological role of nuclear Dp71d; interaction with the nuclear envelope protein emerin

Dp71d associates with lamin B1 in PC12 cells to modulate its cell cycle-associated functions [23]. To investigate additional roles of nuclear Dp71d, we examined the potential interaction of Dp71d with the nuclear envelope protein emerin [65], which has recently been found to be functionally related to β-dystroglycan, a dystrophin-associated protein [66]. Nuclear extracts from PC12 cells were immunoprecipitated with

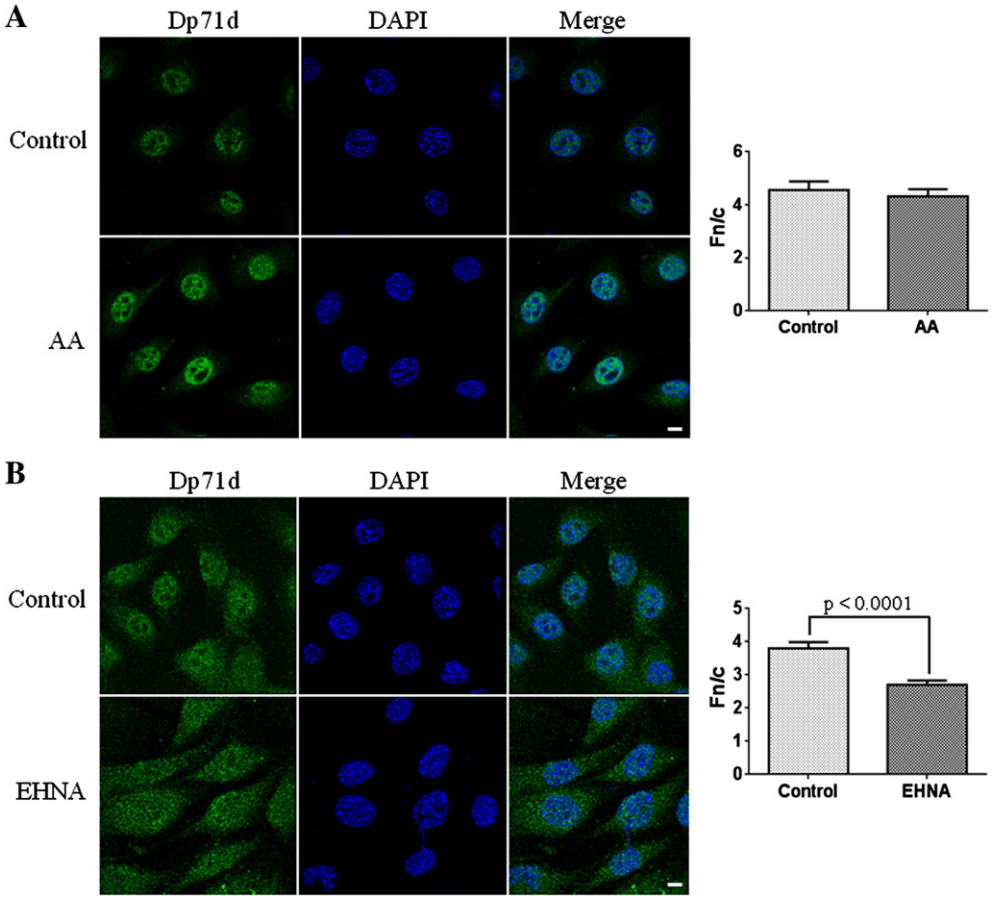

Fig. 9. Dynein-dependent transport facilitates nuclear import of Dp71d. C2C12 cells seeded on glass coverslips were treated with the kinesin inhibitor AA (A) or the dynein inhibitor EHNA (B), diluted in DMSO or H_2O, or with DMSO or H_2O alone (control). Cells were fixed 12 h later, immunostained for Dp71d (green) and counterstained with DAPI (nuclei, blue). Cell preparations were analysed by CLSM and single optical Z-sections are shown. Image analysis was performed as described in the legend to Fig. 1. Results represent the mean +/− SEM (n = 50), with significant differences between control and EHNA-treated cells denoted by the p values.

anti-Dp71d antibodies and analysed by immunoblotting with antibodies directed against emerin or Dp71d itself. Emerin was coimmunoprecipitated with the anti-Dp71d antibody (Fig. 10A), whereas neither protein was recovered after immunoprecipitation using a control antibody (IgG0). Analogously, an anti-emerin antibody was consistently able to coimmunoprecipitate Dp71d. To confirm these results, *in vitro* GST pull down assays were performed using Dp71d expressed as GST fusion in *Escherichia coli* and subsequently purified on glutathione-Sepharose, and emerin produced and labelled *in vitro* with [^{35}S]methionine by a coupled transcription-translation rabbit reticulocyte lysate system. GST-Dp71d immobilised on glutathione-Sepharose beads as per Fig. 6A was incubated with ^{35}S-labelled emerin and interacting complexes were pulled down and analysed by phosphorimaging. As shown in Fig. 10B (top panel), a significant fraction of ^{35}S-emerin was recovered in the precipitate of GST-Dp71d but not in that of GST alone, confirming specific interaction between Dp71d and emerin. To begin to determine the physiological role of Dp71d-emerin interaction, we assessed the effect of Dp71d knockdown on emerin distribution. Lysates from PC12 control (cells stably transfected with an empty vector) and AS1-Dp71 cells (stably transfected with antisense-Dp71 vector) [23] were analysed by Western to evaluate Dp71d levels, with GAPDH as a loading control. Fig. 10C shows a substantial depletion of Dp71 levels in AS1-Dp71 cells, compared with control cells. Interestingly, in parallel with decreased immunostaining for Dp71d in AS1-Dp71 cells, a significant number of the cells (c. 50% compared to only about 20% in the absence of knockdown) showed irregular immunolabelling patterns for emerin, characterised by invaginations of the nuclear envelope, as compared with control cells (Fig. 10D,E), indicating altered nuclear morphology as a result of the reduced levels of Dp71d. The clear implication is that nuclear Dp71d contributes to emerin nuclear envelope localization and nuclear integrity.

4. Discussion

We delineate here for the first time the signal sequences and transporters responsible for the nuclear localisation of dystrophin Dp71d, using the C2C12 cell system as a model. Using various truncation and point mutant derivatives, we show that the ZZ domain, comprising two zinc finger motifs and surrounding amino acid residues, mediates nuclear import of Dp71d. Additionally, an *in vitro* reconstituted nuclear transport assay demonstrates that ZZ-mediated nuclear import of Dp71d is crucially dependent on IMPα2 and β1, consistent with its ability to bind directly with high, nM affinity to the IMPα2/β1 heterodimer. Importantly, complexes of IMPα2/β1 with Dp71d in intact cells could be demonstrated in pull down/IP experiments, while Dp71d nuclear import was also sensitive to agents targeting the NPC (ABL), and the dominant negative Ran mutant RanQ69L. All of these results are consistent with the idea that a conventional, active nuclear import pathway dependent on IMPα2/β1 recognition of ZZ is responsible for Dp71d nuclear localization in intact cells. In addition, it seems clear that binding in the nucleus, potentially mediated by the ZZ based on the results in the presence of CHAPS in our *in vitro* reconstituted nuclear transport system (Fig. 5D,E), may also contribute to Dp71d's nuclear accumulation, as has been noted for several other Zn^{2+}-finger-containing proteins (see below).

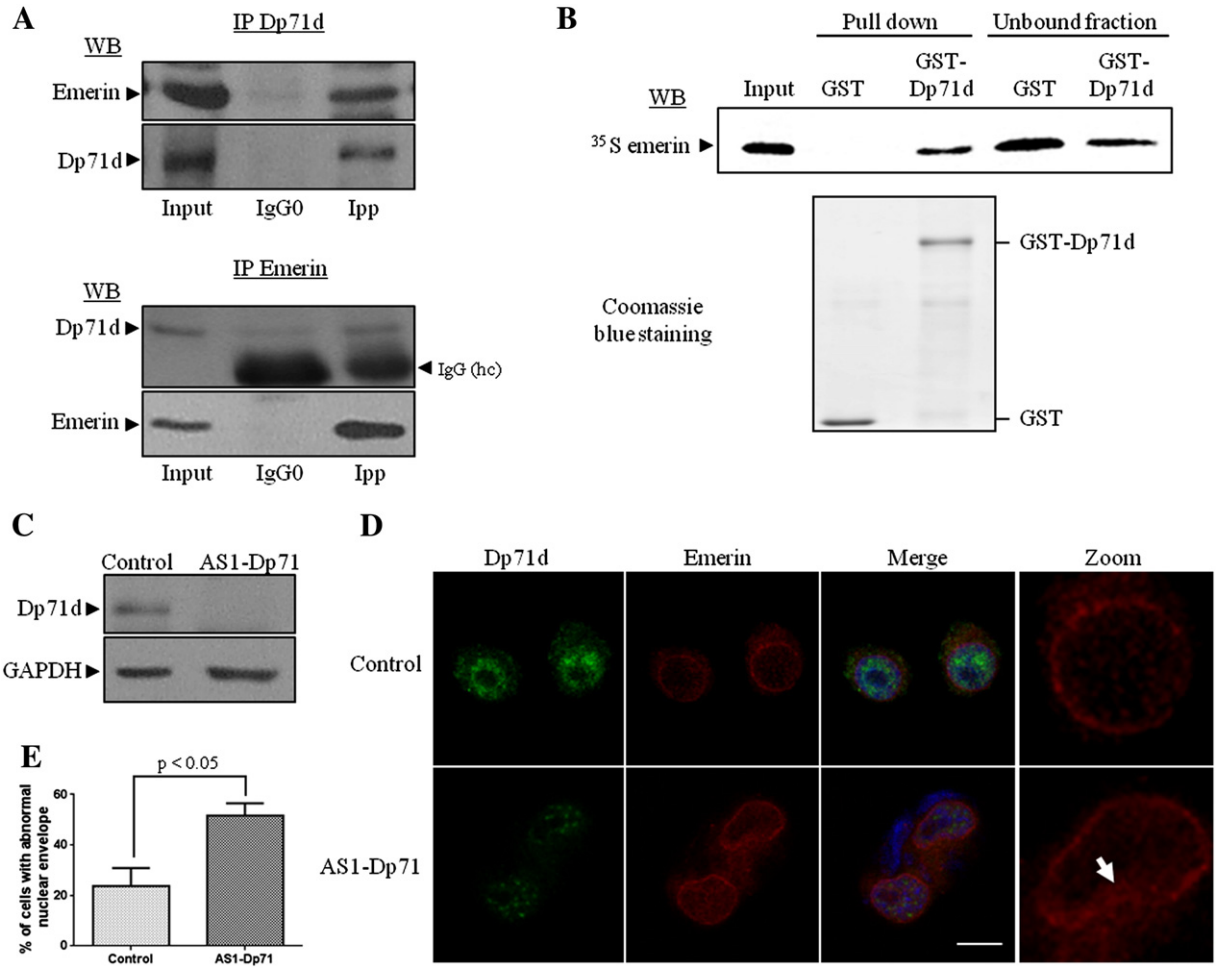

Fig. 10. Dp71d interacts with emerin and Dp71d knockdown alters emerin localization. (A) Nuclear extracts from PC12 control cells were immunoprecipitated with anti-Dp71d or anti-emerin antibodies or with a control antibody (IgG0). Immunoprecipitated proteins were analysed by Western analysis using anti-emerin or -Dp71d antibodies. (B) GST and GST-Dp71d proteins were expressed in *Escherichia coli*, purified using glutathione-Sepharose beads, and visualized by SDS-PAGE followed by Coomassie blue staining (bottom panel). GST and GST-Dp71d proteins immobilised on glutathione-Sepharose beads were incubated with *in vitro* translated ^{35}S emerin to perform affinity pull-down assays. Phosphorimaging results documenting ^{35}S emerin association with GST-Dp71d but not GST alone are shown at the top. The input lane represents 10% of the reticulocyte reaction used in the binding assay. (C) Lysates from control (cells bearing an empty vector) and AS1-Dp71 (cells bearing an antisense-Dp71 vector) clones were subjected to SDS-PAGE/Western analysis with anti-Dp71d and GAPDH (loading control) antibodies. (D) Control and AS1 cells seeded on coverslips were fixed, double stained with anti-Dp71d (green) and -emerin (red) antibodies and counterstained with DAPI to enable nuclei to be visualized (blue), prior to be analysed by CLSM. Single typical optical Z-sections were selected to show distribution of Dp71d and emerin and nuclear envelope morphology. Scale bar, 10 μm. (E) The percentage of cells with abnormal staining of the nuclear envelope is shown. Results represent the mean +/− SEM for 3 separate experiments ($n = 200$ cells), with significant differences between control and AS1-Dp71 cells denoted by the p value.

A number of Zn^{2+}-finger-containing proteins have been described that localise in the nucleus, although the specific role of the Zn^{2+}-finger domains in this context has not always been evident. The NLS of the Zn^{2+}-finger protein Wt1 (Wilm's tumour 1 protein) has been localised to the first (of four) Zn^{2+}-fingers in the protein, and the second of two Zn^{2+}-fingers from TR2 (human testicular receptor 2) is sufficient for nuclear localisation [48,67]. In contrast, the nuclear localising activity of a number of other proteins cannot be ascribed to particular Zn^{2+}-fingers within the respective proteins [49,50,68,69], although mutations that disrupt Zn^{2+}-finger tertiary structure abrogate nuclear localisation of NGFI-A and JAZ [68,69], nuclear import in the case of EKLF/KLF1 appears to be independent of Zn^{2+}-finger structure [50]. In the case of Dp71d, it seems clear that Zn^{2+}-finger structure is essential for the ZZ-dependent nuclear import, since treatment with the Zn^{2+}-chelator TPEN significantly impairs nuclear localisation and site-directed mutagenesis and IPs indicate that the third cysteine in the first Zn^{2+}-finger and second cysteine and histidine residue in the second Zn^{2+}-finger are crucial for IMPα2/β1-mediated nuclear localisation of Dp71d. Based on the results in Fig. 3, however (see Section 3), and the work of others [48,50,55], it is clear that the Dp71d NLS is complex, and almost certainly dependent on other residues within the Zn^{2+}-finger domain in addition to the Zn^{2+}-fingers themselves. More detailed analysis is required in the future to establish this formally, and in particular the interdependence of particular residues within the Zn^{2+}-finger domain, its structural conformation, and IMP recognition.

Although critically dependent on interactions with IMPs, nuclear protein import has also been shown in several cases to be strongly influenced by interactions with cytoskeletal elements [70], with a direct role of the microtubule (MT) network observed in facilitating the nuclear import of specific cancer regulatory proteins, including p53, PTHrP and RB [60,61]. Here we show that the MT-depolymerizing agent nocodazole and the dynein inhibitor EHNA both block nuclear translocation of Dp71d, implying roles for both MT integrity and dynein in Dp71d nuclear transport. Fig. 11 represents a schematic model for Dp71d nuclear translocation, dependent on both MTs/dynein and IMPs. Cytoplasmic Dp71d is normally associated with the plasma membrane within the DAPC; we propose that in response to specific signals such as phosphorylation (see [71,73]), Dp71d may be released from the plasma membrane to be transported through the cytoplasm towards the nucleus through the MT motor protein dynein; subsequently, in the vicinity of the nucleus, the NLS of Dp71d is recognised by IMPα2/β1 to enable passage through the NPC (Fig. 11).

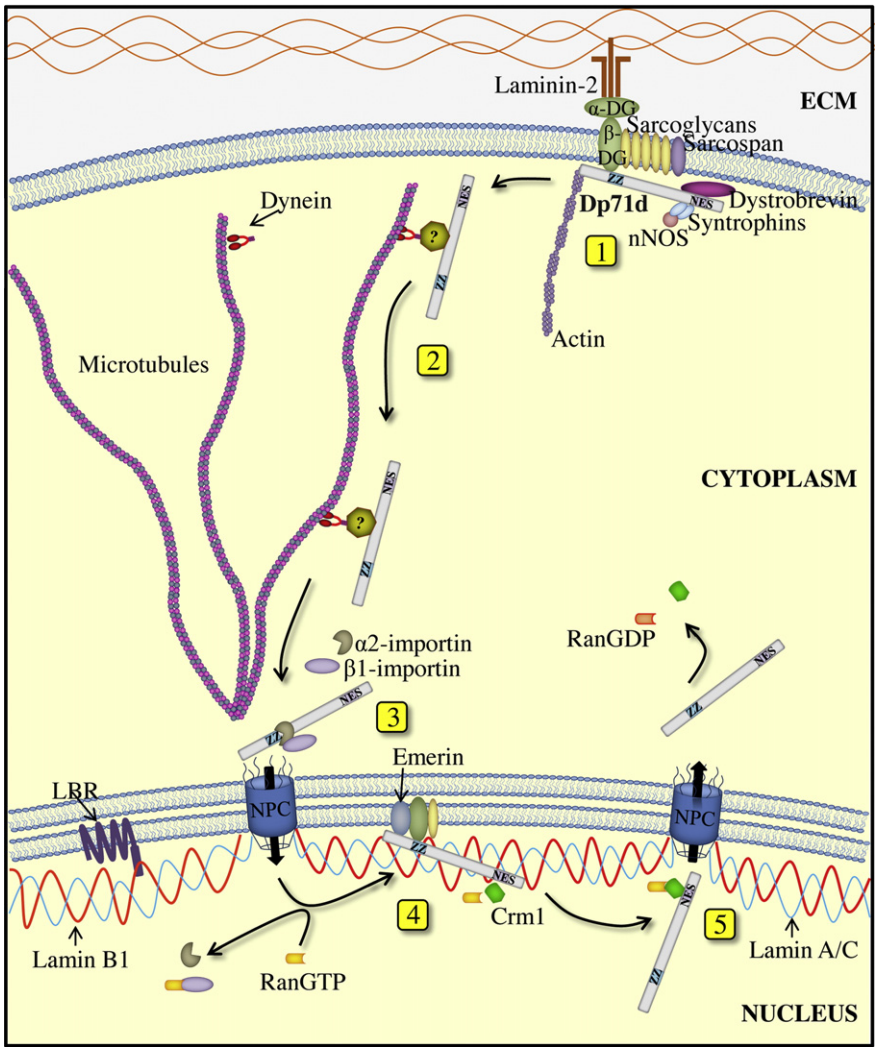

Fig. 11. Proposed model for nucleocytoplasmic shuttling mechanism of Dp71d. Dp71d localises in the cytoplasm within the plasma membrane-localised dystrophin-associated protein complex (DAPC) (1). In response to specific cellular signals such as phosphorylation, Dp71d disassembles from DAPC to be transported retrogradely towards the nucleus via association with the motor protein dynein and microtubules (2). In analogous fashion to other systems [48,67], the IMPα2/β1 heterodimer recognizes the NLS within the ZZ domain of Dp71d near the nuclear periphery, dissociating the protein from dynein and subsequently mediating its nuclear entry via the NPC (3). After RanGTP-mediated release of Dp71d from the import complex, this protein assembles a nuclear DAPC, which is anchored to the nuclear envelope through interaction between Dp71d and both emerin (this study) and lamin B1 (4). A portion of Dp71d is subsequently exported from the nucleus to the cytoplasm via binding of CRM1/RanGTP to Dp71d's NES (5).

Although Dp71d is predominantly nuclear in various different cell types [24,26,30], including those analysed here, its presence in the cytoplasm is critical to the integrity of DAPCs at the plasma membrane [74,78]. The results here implicate Dp71d for the first time as a nucleocytoplasmic shuttling protein, whose cytoplasmic localisation may relate strongly to a CRM1 recognised NES located in the C-terminal domain (amino acids 505–515). Thus, the balance between nuclear import and export pathways is likely to be critical to maintenance of the DAPCs at the plasma membrane, as well as yet undefined nuclear roles of Dp71d.

Dp71d has been found in the nuclear envelope fractions of C2C12 cells [25], and nuclear matrix of HeLa [24] and PC12 cells [79], implying that Dp71d may play a structural role in the nuclear compartment analogous to that at the plasma membrane. Consistent with this idea, Dp71d has been shown to interact in the nucleus with DAPs such as sarcoglycans, β-dystroglycan, syntrophins, and dystrobrevins, to assemble a nuclear DAPC in various cell types [24,25,27]; Dp71d levels appear to impact on the levels of DAPs in the nucleus [27], underlining an important role for nuclear Dp71d, and efficient nuclear import thereof. We previously showed that Dp71d is a component of the mitotic spindle and cytokinesis multiprotein apparati that modulate PC12 cell division by binding to lamin B1, a nuclear envelope protein involved in cell division, with Dp71 knockdown resulting in decreased levels of lamin B1 [23]. Here we show for the first time that Dp71d also binds to the nuclear envelope protein, emerin, both *in vivo* and *in vitro*. Significantly, knockdown of Dp71d results in altered subcellular localization of emerin, with striking impact on nuclear morphology, further supporting the idea that nuclear Dp71d, in part through facilitating the localisation of proteins such as emerin in the nuclear envelope, may be central to a number of critical nuclear processes including nuclei morphology, gene expression, and DNA repair.

In summary, this study identifies functional nuclear targeting sequences within Dp71d for the first time, as well as the transporters that recognize them, and establishes a dependence on microtubule integrity for optimal nuclear accumulation. These previously unrecognised nuclear transport properties are likely to be critical to Dp71d's unique physiological roles in both the cytoplasm and the nucleus, and particularly with respect to maintenance of nuclear architecture.

Supplementary data to this article can be found online at http://dx.doi.org/10.1016/j.bbamcr.2014.01.027.

Acknowledgements

The authors acknowledge the assistance of the facilities of the Unidad de Microscopía Confocal (Centro de Investigación y Estudios Avanzados del IPN) and Monash Microimaging (Monash, Clayton, Vic., Australia) for assistance with microscopy. This study was supported by CONACyT (Mexico; no. 54858 to BC) and the National Health and Medical Research Council (Australia; APP1002486 to DAJ).

References

[1] D.J. Blake, A. Weir, S.E. Newey, K.E. Davies, Function and genetics of dystrophin and dystrophin-related proteins in muscle, Physiol. Rev. 82 (2002) 291–329.
[2] M. Koenig, E.P. Hoffman, C.J. Bertelson, A.P. Monaco, C. Feener, L.M. Kunkel, Complete cloning of the Duchenne muscular dystrophy (DMD) cDNA and preliminary genomic organization of the DMD gene in normal and affected individuals, Cell 50 (1987) 509–517.
[3] F.M. Boyce, A.H. Beggs, C. Feener, L.M. Kunkel, Dystrophin is transcribed in brain from a distant upstream promoter, Proc. Natl. Acad. Sci. U. S. A. 88 (1991) 1276–1280.
[4] E. Holder, M. Maeda, R.D. Bies, Expression and regulation of the dystrophin Purkinje promoter in human skeletal muscle, heart, and brain, Hum. Genet. 97 (1996) 232–239.
[5] H.J. Klamut, S.B. Gangopadhyay, R.G. Worton, P.N. Ray, Molecular and functional analysis of the muscle-specific promoter region of the Duchenne muscular dystrophy gene, Mol. Cell. Biol. 10 (1990) 193–205.
[6] H.G. Lidov, S. Selig, L.M. Kunkel, Dp140: a novel 140 kDa CNS transcript from the dystrophin locus, Hum. Mol. Genet. 4 (1995) 329–335.
[7] J.P. Hugnot, H. Gilgenkrantz, N. Vincent, P. Chafey, G.E. Morris, A.P. Monaco, Y. Berwald-Netter, A. Koulakoff, J.C. Kaplan, A. Kahn, et al., Distal transcript of the dystrophin gene initiated from an alternative first exon and encoding a 75-kDa protein widely distributed in nonmuscle tissues, Proc. Natl. Acad. Sci. U. S. A. 89 (1992) 7506–7510.
[8] T.J. Byers, H.G. Lidov, L.M. Kunkel, An alternative dystrophin transcript specific to peripheral nerve, Nat. Genet. 4 (1993) 77–81.
[9] V.N. D'Souza, T.M. Nguyen, G.E. Morris, W. Karges, D.A. Pillers, P.N. Ray, A novel dystrophin isoform is required for normal retinal electrophysiology, Hum. Mol. Genet. 4 (1995) 837–842.
[10] S. Bar, E. Barnea, Z. Levy, S. Neuman, D. Yaffe, U. Nudel, A novel product of the Duchenne muscular dystrophy gene which greatly differs from the known isoforms in its structure and tissue distribution, Biochem. J. 272 (1990) 557–560.
[11] D.J. Blake, D.R. Love, J. Tinsley, G.E. Morris, H. Turley, K. Gatter, G. Dickson, Y.H. Edwards, K.E. Davies, Characterization of a 4.8 kb transcript from the Duchenne muscular dystrophy locus expressed in Schwannoma cells, Hum. Mol. Genet. 1 (1992) 103–109.
[12] S.L. Morales-Lazaro, R. Gonzalez-Ramirez, P. Gomez, V. Tapia-Ramirez, M.B. de Leon, B. Cisneros, Induction of dystrophin Dp71 expression during neuronal differentiation: opposite roles of Sp1 and AP2alpha in Dp71 promoter activity, J. Neurochem. 112 (2010) 474–485.
[13] M.B. de Leon, C. Montanez, P. Gomez, S.L. Morales-Lazaro, V. Tapia-Ramirez, V. Valadez-Graham, F. Recillas-Targa, D. Yaffe, U. Nudel, B. Cisneros, Dystrophin Dp71 expression is down-regulated during myogenesis: role of Sp1 and Sp3 on the Dp71 promoter activity, J. Biol. Chem. 280 (2005) 5290–5299.
[14] D. Lederfein, Z. Levy, N. Augier, D. Mornet, G. Morris, O. Fuchs, D. Yaffe, U. Nudel, A 71-kilodalton protein is a major product of the Duchenne muscular dystrophy gene in brain and other nonmuscle tissues, Proc. Natl. Acad. Sci. U. S. A. 89 (1992) 5346–5350.
[15] F. Daoud, N. Angeard, B. Demerre, I. Martie, R. Benyaou, F. Leturcq, M. Cossee, N. Deburgrave, Y. Saillour, S. Tuffery, A. Urtizberea, A. Toutain, B. Echenne, M. Frischman, M. Mayer, I. Desguerre, B. Estournet, C. Reveillere, B. Penisson, J.M. Cuisset, J.C. Kaplan, D. Heron, F. Rivier, J. Chelly, Analysis of Dp71 contribution in the severity of mental retardation through comparison of Duchenne and Becker patients differing by mutation consequences on Dp71 expression, Hum. Mol. Genet. 18 (2009) 3779–3794.
[16] M.P. Moizard, A. Toutain, D. Fournier, F. Berret, M. Raynaud, C. Billard, C. Andres, C. Moraine, Severe cognitive impairment in DMD: obvious clinical indication for Dp71 isoform point mutation screening, Eur. J. Hum. Genet. 8 (2000) 552–556.
[17] R. Tadayoni, A. Rendon, L.E. Soria-Jasso, B. Cisneros, Dystrophin dp71: the smallest but multifunctional product of the Duchenne muscular dystrophy gene, Mol. Neurobiol. 45 (2012) 43–60.
[18] C. Dalloz, R. Sarig, P. Fort, D. Yaffe, A. Bordais, T. Pannicke, J. Grosche, D. Mornet, A. Reichenbach, J. Sahel, U. Nudel, A. Rendon, Targeted inactivation of dystrophin gene product Dp71: phenotypic impact in mouse retina, Hum. Mol. Genet. 12 (2003) 1543–1554.
[19] P.E. Fort, A. Sene, T. Pannicke, M.J. Roux, V. Forster, D. Mornet, U. Nudel, D. Yaffe, A. Reichenbach, J.A. Sahel, A. Rendon, Kir4.1 and AQP4 associate with Dp71- and utrophin-DAPs complexes in specific and defined microdomains of Muller retinal glial cell membrane, Glia 56 (2008) 597–610.
[20] J. Cerna, J.A. Osuna-Castro, J. Muniz, D. Mornet, F. Garcia-Sierra, B. Cisneros, Dystrophin Dp71f associates with components of the beta1-integrin adhesion complex in PC12 cell neurites, Acta Neurol. Belg. 109 (2009) 132–135.
[21] J.A. Enriquez-Aragon, J. Cerna-Cortes, M. Bermudez de Leon, F. Garcia-Sierra, E. Gonzalez, D. Mornet, B. Cisneros, Dystrophin Dp71 in PC12 cell adhesion, Neuroreport 16 (2005) 235–238.
[22] J. Cerna, D. Cerecedo, A. Ortega, F. Garcia-Sierra, F. Centeno, E. Garrido, D. Mornet, B. Cisneros, Dystrophin Dp71f associates with the beta1-integrin adhesion complex to modulate PC12 cell adhesion, J. Mol. Biol. 362 (2006) 954–965.
[23] M. Villarreal-Silva, F. Centeno-Cruz, R. Suarez-Sanchez, E. Garrido, B. Cisneros, Knockdown of dystrophin Dp71 impairs PC12 cells cycle: localization in the spindle and cytokinesis structures implies a role for Dp71 in cell division, PLoS One 6 (2011) e23504.
[24] L. Fuentes-Mera, R. Rodriguez-Munoz, R. Gonzalez-Ramirez, F. Garcia-Sierra, E. Gonzalez, D. Mornet, B. Cisneros, Characterization of a novel Dp71 dystrophin-associated protein complex (DAPC) present in the nucleus of HeLa cells: members of the nuclear DAPC associate with the nuclear matrix, Exp. Cell Res. 312 (2006) 3023–3035.
[25] R. Gonzalez-Ramirez, S.L. Morales-Lazaro, V. Tapia-Ramirez, D. Mornet, B. Cisneros, Nuclear and nuclear envelope localization of dystrophin Dp71 and dystrophin-associated proteins (DAPs) in the C2C12 muscle cells: DAPs nuclear localization is modulated during myogenesis, J. Cell. Biochem. 105 (2008) 735–745.
[26] V. Aleman, B. Osorio, O. Chavez, A. Rendon, D. Mornet, D. Martinez, Subcellular localization of Dp71 dystrophin isoforms in cultured hippocampal neurons and forebrain astrocytes, Histochem. Cell Biol. 115 (2001) 243–254.
[27] M. Villarreal-Silva, R. Suarez-Sanchez, R. Rodriguez-Munoz, D. Mornet, B. Cisneros, Dystrophin Dp71 is critical for stability of the DAPs in the nucleus of PC12 cells, Neurochem. Res. 35 (2010) 366–373.
[28] R. Acosta, C. Montanez, L. Fuentes-Mera, E. Gonzalez, P. Gomez, L. Quintero-Mora, D. Mornet, L.M. Alvarez-Salas, B. Cisneros, Dystrophin Dp71 is required for neurite outgrowth in PC12 cells, Exp. Cell Res. 296 (2004) 265–275.
[29] E. Gonzalez, C. Montanez, P.N. Ray, P.L. Howard, F. Garcia-Sierra, D. Mornet, B. Cisneros, Alternative splicing regulates the nuclear or cytoplasmic localization of dystrophin Dp71, FEBS Lett. 482 (2000) 209–214.
[30] F.G. Marquez, B. Cisneros, F. Garcia, V. Ceja, F. Velazquez, F. Depardon, L. Cervantes, A. Rendon, D. Mornet, H. Rosas-vargas, M. Mustre, C. Montanez, Differential expression and subcellular distribution of dystrophin Dp71 isoforms during differentiation process, Neuroscience 118 (2003) 957–966.
[31] D.A. Jans, C.Y. Xiao, M.H. Lam, Nuclear targeting signal recognition: a key control point in nuclear transport? Bioessays 22 (2000) 532–544.
[32] L.F. Pemberton, B.M. Paschal, Mechanisms of receptor-mediated nuclear import and nuclear export, Traffic 6 (2005) 187–198.
[33] R.C. Austin, P.L. Howard, V.N. D'Souza, H.J. Klamut, P.N. Ray, Cloning and characterization of alternatively spliced isoforms of Dp71, Hum. Mol. Genet. 4 (1995) 1475–1483.
[34] C. Beetz, M. Brodhun, K. Moutzouris, M. Kiehntopf, A. Berndt, D. Lehnert, T. Deufel, M. Bastmeyer, J. Schickel, Identification of nuclear localisation sequences in spastin (SPG4) using a novel Tetra-GFP reporter system, Biochem. Biophys. Res. Commun. 318 (2004) 1079–1084.
[35] S. Hubner, C.Y. Xiao, D.A. Jans, The protein kinase CK2 site (Ser111/112) enhances recognition of the simian virus 40 large T-antigen nuclear localization sequence by importin, J. Biol. Chem. 272 (1997) 17191–17195.
[36] B.C. Baliga, P.A. Colussi, S.H. Read, M.M. Dias, D.A. Jans, S. Kumar, Role of prodomain in importin-mediated nuclear localization and activation of caspase-2, J. Biol. Chem. 278 (2003) 4899–4905.
[37] D.W. Heilman, J.G. Teodoro, M.R. Green, Apoptin nucleocytoplasmic shuttling is required for cell type-specific localization, apoptosis, and recruitment of the anaphase-promoting complex/cyclosome to PML bodies, J. Virol. 80 (2006) 7535–7545.
[38] C.G. Garcia-Tovar, A. Perez, J. Luna, R. Mena, B. Osorio, V. Aleman, R. Mondragon, D. Mornet, A. Rendon, J.M. Hernandez, Biochemical and histochemical analysis of 71 kDa dystrophin isoform (Dp71f) in rat brain, Acta Histochem. 103 (2001) 209–224.
[39] D.A. Jans, T. Moll, K. Nasmyth, P. Jans, Cyclin-dependent kinase site-regulated signal-dependent nuclear localization of the SW15 yeast transcription factor in mammalian cells, J. Biol. Chem. 270 (1995) 17064–17067.
[40] A. Argentaro, H. Sim, S. Kelly, S. Preiss, A. Clayton, D.A. Jans, V.R. Harley, A SOX9 defect of calmodulin-dependent nuclear import in campomelic dysplasia/autosomal sex reversal, J. Biol. Chem. 278 (2003) 33839–33847.
[41] B. Lara-Chacon, M.B. de Leon, D. Leocadio, P. Gomez, L. Fuentes-Mera, I. Martinez-Vieyra, A. Ortega, D.A. Jans, B. Cisneros, Characterization of an Importin alpha/beta-recognized nuclear localization signal in beta-dystroglycan, J. Cell. Biochem. 110 (2010) 706–717.
[42] R. Ghildyal, A. Ho, K.M. Wagstaff, M.M. Dias, C.L. Barton, P. Jans, P. Bardin, D.A. Jans, Nuclear import of the respiratory syncytial virus matrix protein is mediated by importin beta1 independent of importin alpha, Biochemistry 44 (2005) 12887–12895.
[43] K.M. Wagstaff, D.A. Jans, Intramolecular masking of nuclear localization signals: analysis of importin binding using a novel AlphaScreen-based method, Anal. Biochem. 348 (2006) 49–56.
[44] A.C. Hearps, D.A. Jans, HIV-1 integrase is capable of targeting DNA to the nucleus via an importin alpha/beta-dependent mechanism, Biochem. J. 398 (2006) 475–484.
[45] A. Efthymiadis, L.J. Briggs, D.A. Jans, The HIV-1 Tat nuclear localization sequence confers novel nuclear import properties, J. Biol. Chem. 273 (1998) 1623–1628.
[46] J.K. Forwood, V. Harley, D.A. Jans, The C-terminal nuclear localization signal of the sex-determining region Y (SRY) high mobility group domain mediates nuclear import through importin beta 1, J. Biol. Chem. 276 (2001) 46575–46582.
[47] R. Lixin, A. Efthymiadis, B. Henderson, D.A. Jans, Novel properties of the nucleolar targeting signal of human angiogenin, Biochem. Biophys. Res. Commun. 284 (2001) 185–193.
[48] W. Bruening, P. Moffett, S. Chia, G. Heinrich, J. Pelletier, Identification of nuclear localization signals within the zinc fingers of the WT1 tumor suppressor gene product, FEBS Lett. 393 (1996) 41–47.

[49] H. Yamasaki, T. Sekimoto, T. Ohkubo, T. Douchi, Y. Nagata, M. Ozawa, Y. Yoneda, Zinc finger domain of Snail functions as a nuclear localization signal for importin beta-mediated nuclear import pathway, Genes Cells 10 (2005) 455–464.
[50] K. Pandya, T.M. Townes, Basic residues within the Kruppel zinc finger DNA binding domains are the critical nuclear localization determinants of EKLF/KLF-1, J. Biol. Chem. 277 (2002) 16304–16312.
[51] E. Saijou, T. Itoh, K.W. Kim, S. Iemura, T. Natsume, A. Miyajima, Nucleocytoplasmic shuttling of the zinc finger protein EZI Is mediated by importin-7-dependent nuclear import and CRM1-independent export mechanisms, J. Biol. Chem. 282 (2007) 32327–32337.
[52] T. Ito, M. Azumano, C. Uwatoko, K. Itoh, J. Kuwahara, Role of zinc finger structure in nuclear localization of transcription factor Sp1, Biochem. Biophys. Res. Commun. 380 (2009) 28–32.
[53] K. Hnia, D. Zouiten, S. Cantel, D. Chazalette, G. Hugon, J.A. Fehrentz, A. Masmoudi, A. Diment, J. Bramham, D. Mornet, S.J. Winder, ZZ domain of dystrophin and utrophin: topology and mapping of a beta-dystroglycan interaction site, Biochem. J. 401 (2007) 667–677.
[54] A. Pokorska, C. Drevet, C. Scazzocchio, The analysis of the transcriptional activator PrnA reveals a tripartite nuclear localisation sequence, J. Mol. Biol. 298 (2000) 585–596.
[55] M. Hatayama, T. Tomizawa, K. Sakai-Kato, P. Bouvagnet, S. Kose, N. Imamoto, S. Yokoyama, N. Utsunomiya-Tate, K. Mikoshiba, T. Kigawa, J. Aruga, Functional and structural basis of the nuclear localization signal in the ZIC3 zinc finger domain, Hum. Mol. Genet. 17 (2008) 3459–3473.
[56] L.G. Yu, D.G. Fernig, M.R. White, D.G. Spiller, P. Appleton, R.C. Evans, I. Grierson, J.A. Smith, H. Davies, O.V. Gerasimenko, O.H. Petersen, J.D. Milton, J.M. Rhodes, Edible mushroom (*Agaricus bisporus*) lectin, which reversibly inhibits epithelial cell proliferation, blocks nuclear localization sequence-dependent nuclear protein import, J. Biol. Chem. 274 (1999) 4890–4899.
[57] A.V. Sorokin, E.R. Kim, L.P. Ovchinnikov, Nucleocytoplasmic transport of proteins, Biochemistry (Mosc) 72 (2007) 1439–1457.
[58] S.R. Wente, M.P. Rout, The nuclear pore complex and nuclear transport, Cold Spring Harb. Perspect. Biol. 2 (2010) a000562.
[59] A. Efthymiadis, H. Shao, S. Hubner, D.A. Jans, Kinetic characterization of the human retinoblastoma protein bipartite nuclear localization sequence (NLS) *in vivo* and *in vitro*. A comparison with the SV40 large T-antigen NLS, J. Biol. Chem. 272 (1997) 22134–22139.
[60] D.M. Roth, G.W. Moseley, D. Glover, C.W. Pouton, D.A. Jans, A microtubule-facilitated nuclear import pathway for cancer regulatory proteins, Traffic 8 (2007) 673–686.
[61] D.M. Roth, G.W. Moseley, C.W. Pouton, D.A. Jans, Mechanism of microtubule-facilitated "fast track" nuclear import, J. Biol. Chem. 286 (2011) 14335–14351.
[62] X. Gong, X. Ming, P. Deng, Y. Jiang, Mechanisms regulating the nuclear translocation of p38 MAP kinase, J. Cell. Biochem. 110 (2010) 1420–1429.
[63] I. Mikenberg, D. Widera, A. Kaus, B. Kaltschmidt, C. Kaltschmidt, Transcription factor NF-kappaB is transported to the nucleus via cytoplasmic dynein/dynactin motor complex in hippocampal neurons, PLoS One 2 (2007) e589.
[64] G.W. Moseley, D.M. Roth, M.A. DeJesus, D.L. Leyton, R.P. Filmer, C.W. Pouton, D.A. Jans, Dynein light chain association sequences can facilitate nuclear protein import, Mol. Biol. Cell 18 (2007) 3204–3213.
[65] J.M. Berk, K.E. Tifft, K.L. Wilson, The nuclear envelope LEM-domain protein emerin, Nucleus 4 (2013) 1–17.
[66] I.A. Martinez-Vieyra, A. Vasquez-Limeta, R. Gonzalez-Ramirez, S.L. Morales-Lazaro, M. Mondragon, R. Mondragon, A. Ortega, S.J. Winder, B. Cisneros, A role for beta-dystroglycan in the organization and structure of the nucleus in myoblasts, Biochim. Biophys. Acta 1833 (2013) 698–711.
[67] Z. Yu, C.H. Lee, C. Chinpaisal, L.N. Wei, A constitutive nuclear localization signal from the second zinc-finger of orphan nuclear receptor TR2, J. Endocrinol. 159 (1998) 53–60.
[68] M. Yang, W.S. May, T. Ito, JAZ requires the double-stranded RNA-binding zinc finger motifs for nuclear localization, J. Biol. Chem. 274 (1999) 27399–27406.
[69] C. Matheny, M.L. Day, J. Milbrandt, The nuclear localization signal of NGFI-A is located within the zinc finger DNA binding domain, J. Biol. Chem. 269 (1994) 8176–8181.
[70] C.W. Pouton, K.M. Wagstaff, D.M. Roth, G.W. Moseley, D.A. Jans, Targeted delivery to the nucleus, Adv. Drug Deliv. Rev. 59 (2007) 698–717.
[71] L. Calderilla-Barbosa, A. Ortega, B. Cisneros, Phosphorylation of dystrophin Dp71d by Ca2+/calmodulin-dependent protein kinase II modulates the Dp71d nuclear localization in PC12 cells, J. Neurochem. 98 (2006) 713–722.
[72] A. Kaffman, E.K. O'Shea, Regulation of nuclear localization: a key to a door, Annu. Rev. Cell Dev. Biol. 15 (1999) 291–339.
[73] T.R. Kau, J.C. Way, P.A. Silver, Nuclear transport and cancer: from mechanism to intervention, Nat. Rev. Cancer 4 (2004) 106–117.
[74] J. Romo-Yanez, V. Ceja, R. Ilarraza-Lomeli, R. Coral-Vazquez, F. Velazquez, D. Mornet, A. Rendon, C. Montanez, Dp71ab/DAPs complex composition changes during the differentiation process in PC12 cells, J. Cell. Biochem. 102 (2007) 82–97.
[75] D.J. Blake, R. Hawkes, M.A. Benson, P.W. Beesley, Different dystrophin-like complexes are expressed in neurons and glia, J. Cell Biol. 147 (1999) 645–658.
[76] T. Claudepierre, C. Dalloz, D. Mornet, K. Matsumura, J. Sahel, A. Rendon, Characterization of the intermolecular associations of the dystrophin-associated glycoprotein complex in retinal Muller glial cells, J. Cell Sci. 113 (Pt 19) (2000) 3409–3417.
[77] T. Haenggi, A. Soontornmalai, M.C. Schaub, J.M. Fritschy, The role of utrophin and Dp71 for assembly of different dystrophin-associated protein complexes (DPCs) in the choroid plexus and microvasculature of the brain, Neuroscience 129 (2004) 403–413.
[78] D. Cerecedo, B. Cisneros, P. Gomez, I.J. Galvan, Distribution of dystrophin- and utrophin-associated protein complexes during activation of human neutrophils, Exp. Hematol. 38 (2010) 618–628(e613).
[79] R. Rodriguez-Munoz, M. Villarreal-Silva, R. Gonzalez-Ramirez, F. Garcia-Sierra, M. Mondragon, R. Mondragon, J. Cerna, B. Cisneros, Neuronal differentiation modulates the dystrophin Dp71d binding to the nuclear matrix, Biochem. Biophys. Res. Commun. 375 (2008) 303–307.
[80] F. Rivier, A. Robert, G. Hugon, A. Bonet-Kerrache, V. Nigro, J.A. Fehrentz, J. Martinez, D. Mornet, Dystrophin and utrophin complexed with different associated proteins in cardiac Purkinje fibres, Histochem. J. 31 (1999) 425–432.